Int J Earth Sci (Geol Rundsch) (2013) 102:1811–1835
DOI 10.1007/s00531-012-0806-z

ORIGINAL PAPER

Channel flow extrusion model to constrain dynamic viscosity and Prandtl number of the Higher Himalayan Shear Zone

Soumyajit Mukherjee

Received: 13 October 2011 / Accepted: 30 June 2012 / Published online: 18 August 2012

Abstract Constraining magnitudes of mechanical and thermo-mechanical parameters of rocks and shear zones are the important goals in structural geology and tectonics (Talbot in J Struct Geol 21:949–957, 1999). Such parameters aid dynamic scaling of analogue tectonic models (Ramberg in Gravity, deformation and the Earth's crust in theory, experiments and geological applications, 2nd edn. Academic Press, London, 1981), which are useful to unravel tectonics in further details (Schultz-Ela and Walsh in J Struct Geol 24:247–275, 2002). The channel flow extrusion of the Higher Himalayan Shear Zone (HHSZ, = Higher Himalaya) can be explained by a top-to-S/SW simple shear (i.e. the D_2 deformation) in combination with a pressure gradient induced flow against gravity. Presuming its Newtonian incompressible rheology with parallel inclined boundaries, the viscosity (μ) of this shear zone along a part of the Himalayan chain through India, Nepal and Bhutan is estimated to vary widely between $\sim 10^{16}$ and 10^{23} Pa s, and its Prandtl number (P_r) within $\sim 10^{21}$–10^{28}. The estimates utilized ranges of known thickness (6–58 km) of the HHSZ, that of its top subzone of ductile shear of normal shear sense ($STDS_U$: 0.35–9.4 km), total rate of slip of its two boundaries (0.7–131 mm year^{-1}), pressure gradient (0.02–6 kb km^{-1}), density (2.2–3.1 g cm^{-3}) and thermal diffusivity (0.5×10^{-6}–2.1×10^{-6} m s^{-2}) along the orogenic trend. Considering most of the parameters specifically for the Sutlej section (India), the calculated viscosity (μ) and the Prandtl number (P_r) of the HHSZ are deduced to be μ: $\sim 10^{17}$–10^{23} Pa s and $P_r \sim 10^{22}$–10^{28}. The upper limits of the estimated viscosity ranges are broadly in conformity with a strong Tibetan mid-crust from where a part of the HHSZ rocks extruded. On the other hand, their complete ranges match with those for its constituent main rock types and partly with those for the superstructure and the infrastructure. The estimated mechanical and thermo-mechanical parameters of the HHSZ will help to build dynamically scaled analogue models for the Himalayan deformation of the D_2–phase.

Keywords Channel flow · Shear zone · Viscosity · Prandtl number · Higher Himalaya · Higher Himalayan Shear Zone · Extrusion

S. Mukherjee (✉)
Department of Earth Sciences, Indian Institute of Technology Bombay, Powai, Mumbai 400 076, Maharashtra, India
e-mail: soumyajitm@gmail.com

Introduction

> *'As in other fields of knowledge the main approaches in Geology to find explanations and understand the mechanics behind geological phenomena have been three: analytical, physical and numerical modeling.'—F. O. Marques* (2012)

Due to its several critical structural, tectonic and metamorphic characters, the Higher Himalayan segment of the entire Himalayan orogen (Fig. 1a, b) has received enormous global attention (e.g. Yin 2006; Hatzfeld and Molnar 2010). Ever since the landmark paper by Beaumont et al. (2001) on coupled thermal–mechanical channel flow extrusion of the Higher Himalaya was published, there has been an intense debate on the validity and modifications of this extrusion mechanism ('Appendix 1'; also see Grujic et al. 1996). The channel flow model envisages tectonic and/or climate controlled flow of partially molten rocks through an inclined channel (the Higher Himalaya) either in a single or in two pulses within ~22–16 Ma (Hollister and Grujic 2006). One of the major structural constraints

that extensional ductile shear within the upper portion of the Higher Himalaya took place simultaneous to the ductile compressional shear within the base is explained efficiently by the channel flow model. A linked subhorizontal feeder channel at a mid-crustal depth still exists below the southern Tibet (Fig. 1c; Beaumont et al. 2001, 2004, 2007; Jamieson et al. 2004, 2006; Hollister and Grujic 2006; also reviews by Burbank 2005; Mukherjee 2005, 2007; 2010a, b, c; Godin et al. 2006; Grujic 2006; Hodges 2006; Jones et al. 2006; Yin 2006; Harris 2007, 2008; Dewei 2008; Mukherjee and Koyi 2010a, b; Searle et al. 2010; Streule et al. 2010; Chen et al. 2011; Jamieson et al. 2011; Imayama et al. 2011; Searle et al. 2011; Burbank and Anderson 2012; Chatterjee et al. 2012; Mukherjee et al. 2012; Mukherjee and Mukherjee 2012; Streule et al. 2012; Yakymchuk et al. 2012).

The channel flow model—as a combination of Couette and Poiseuille flow (Fig. 2)—has been applied in various modified forms over a vast spatial extent along the Himalayan chain—in the western—(Warren et al. 2008a, b, c; Beaumont et al. 2009; Mukherjee 2010a, b, 2012a, b; Mukherjee and Koyi 2010a, b; Mukherjee and Mulchrone 2012), and in the central, eastern, and the far eastern Himalaya (Godin et al. 2006; Jessup et al. 2006; Searle et al. 2006; Zhu et al. 2010; Guilmette et al. 2011; Gong et al. 2012; Zhang et al. 2012). Thus, it appears that the channel flow acted along the entire Himalayan chain but excluding the two syntaxes due to a lack of leucogranite melt at the upper structural level of the HHSZ (Searle and Treloar 2010; Johnson and Harley 2012).

Since the Higher Himalaya has been reported to have undergone a top-to-S/SW sense of ductile shearing (the D_2 deformation event of Jain et al. 2002, also see Mukherjee 2012c, d, e) as revealed most profusely by S–C fabrics, the terrain has been referred as the 'Higher Himalayan Shear Zone' since 1988 (Jain and Anand 1988; Mukherjee 2007, 2010a, b; Mukherjee and Koyi 2010a, b; Mukherjee et al. 2012). Different parts of the HHSZ might have evolved with finally different thermobarometric histories (compare review by Jain et al. 2002 and Yin 2006 with Carosi et al. 2010). Alternative perspectives on their tectonics have been indicated by referring the Higher Himalaya as an 'orogenic wedge' (Grasemann et al. 1999), a 'Higher Himalayan Crystalline Sequence' (Vannay and Grasemann 2001; Vannay et al. 2004), an 'orogenic channel' (Beaumont et al. 2001), a 'Greater Himalayan Sequence' (Grujic et al. 1996, 2002) and a 'Higher Himalayan Slab' (Searle and Szulc 2005). This work describes the Higher Himalaya as a shear zone, that is, it uses the phrase 'Higher Himalayan Shear Zone' (HHSZ) as a synonym for the 'Higher Himalaya'. That different subzones inside the 'HHSZ' were reactivated at different time spans and that there are few undeformed subzones inside it are also appreciated.

While viscosity, a mechanical parameter, measures for internal resistance of a fluid to flow, the Prandtl number (P_r)—a unitless thermo-mechanical parameter (Fowler 2005)—represents how fast heat diffuses from a body compared to its loss in momentum (Schlichting and Gersten 1999). Whereas viscosity can be described as internal friction of fluids to flow, a $P_r \geq 10$ of a 'virtually infinite' magnitude indicates negligible inertial force (Marsh 1989; Lowrie 2007). A $P_r > 1$ indicates a faster diffusion of momentum than heat (Jaupart and Mareschal 2011). As for example, water has a P_r of 8.1 (Turcotte and Schubert 2002). A higher P_r of a fluid in general indicates a thinner thermal boundary layer (Oswald 2009). The P_r is also one of the factors that governs thermal convection (Scheidegger 1982a, b). Incorporation of thermal parameters for the rocks as far as nearer to the natural prototype is needed to generate realistic models (e.g. Maierová et al. 2012).

This work aims to estimate the dynamic viscosity and the Prandtl number of the Higher Himalaya during its channel flow (Fig. 2) by taking account a range of magnitudes for its (i) geometry, (ii) size and (iii) physical properties of the constituent rocks; (iv) slip rates of its boundaries (the Main Central Thrust Zone: MCTZ, and the South Tibetan Detachment System-Upper: $STDS_U$); and (v) the thickness of the $STDS_U$. In one particular case, many of those parameters from one of the well-studied transects of the Sutlej section of the Higher Himalaya (India) were used to calculate a section-specific viscosity and a Prandtl number. These results were then compared with standard values for the rocks that constitute the HHSZ. The present work therefore considers only the channel flow model and makes no attempt to evaluate the suitability of any alternate extrusion models of the Higher Himalaya—most notably the critical taper mechanism. This work does not aim to establish any along strike variation of tectonic parameters in the orogen (Grujic et al. 2004; Carter and Foster 2009; Roberts et al. 2011a, b; Arora et al. 2012; Giambiagi et al. 2012; Johnson and Harley 2012; Mouthereau et al. 2012 etc.) in the Himalaya (i.e. unlike review of Hindle 2003).

Geology and tectonics—Higher Himalayan Shear Zone (HHSZ)

The Himalayan mountain chain is a manifestation of continent–continent collision between the Indian and the Eurasian plates since their collision ~55 Ma onwards. Since then, crustal shortening along the chain, deduced from cross-section balancing, varied from ~500 to 1,000 km under a variable rate of shortening of 10–20 mm $year^{-1}$ (reviews by Piffner 2006; Yin 2010; Long et al. 2011). The mountain developed either by

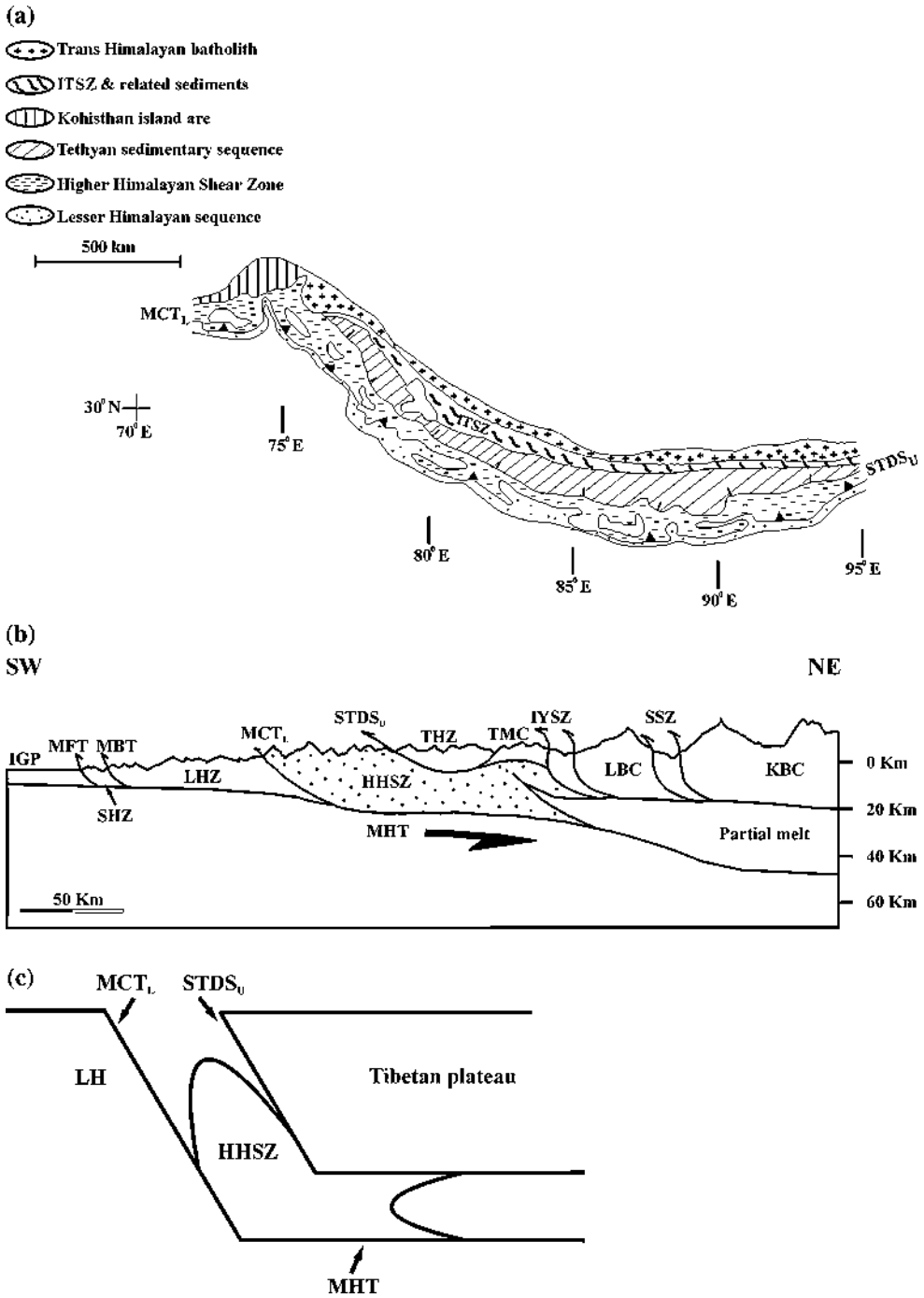

Fig. 1 **a** The Himalayan mountain chain as a number of longitudinal stripes of lithologies (reproduced from fig. 1 of Godin et al. 2006). The 'Greater Himalayan Sequence' of Godin et al. (2006) is presented here as the Higher Himalayan Shear Zone (HHSZ), and their 'Main Central Thrust Zone' as the 'Main Central Thrust-Lower' (MCT_L). **b** A simplified NE–SW cross-section of the Himalaya (reproduced from fig. 1 of Leech et al. 2005). Abbreviations: IGP, Indo Gangetic Plane; MFT, Main Frontal Thrust; SHZ, Sub Himalayan Zone; MBT, Main Boundary Thrust; LHZ, Lesser Himalayan Zone; MCT_L, Main Central Thrust-Lower; HHSZ, Higher Himalayan Shear Zone; MHT, Main Himalayan Thrust; $STDS_U$, South Tibetan Detachment System-Upper; THZ, Tethyan Himalayan Zone; TMC, Tso Morari Crystallines; IYSZ, Indus Yarlung Suture Zone; LBC, Ladakh Batholith Complex; SSZ, Shyok Suture Zone; KBC, Karakoram Batholith Complex. Notice that the Greater Himalayan Zone (GHZ) of Leech et al. (2005) is written here as the Higher Himalayan Shear Zone (HHSZ), Main Central Thrust (MCT) as the MCT_L and the South Tibetan Detachment System ($STDS_U$) as the South Tibetan Detachment System-Upper ($STDS_U$). **c** Schematic presentation of channel flow extrusion of the Higher Himalayan Shear Zone (HHSZ). Parabolas represent velocity profiles. MHT, Main Himalayan Thrust; $STDS_U$, South Tibetan Detachment System-Upper; MCT_L, Main Central Thrust-Lower; neither to scale nor angle. Reproduced from fig. 12a of Mukherjee et al. (2012)

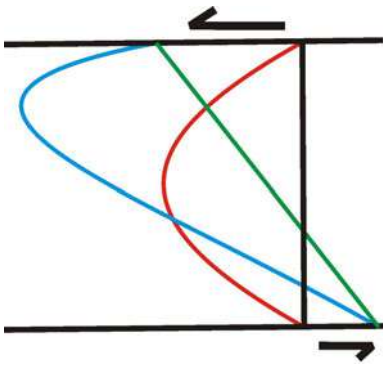

Fig. 2 Velocity profiles for a channel flow: *red* parabola: Poiseuille flow; *green straight line*: Couette flow or simple shear; *blue* parabola: a combination of Couette flow and Poiseuille flow

progressive accretion or by 'protracted' (continuous?) deformation (White and Lister 2012's review; also see fig. 2 of Streule et al. 2010). Inside a sub-horizontal channel with the base defined by the Main Himalayan Thrust, the mid-crustal rocks (~10–30 km depth) of the Tibetan plateau are partially molten to 5–14 % by volume, and persists as a 'jelly-sandwich model' (Johnson and Harley 2012) where the viscosity falls drastically up to three order of magnitudes (Liu and Yang 2003; as reproduced in fig. 10.26 of Keary et al. 2009). The subhorizontal channel defines a flat segment of the channel that links to the inclined HHSZ ramp where there is only 2–4 % by volume partial melt (Fig. 1c; Beaumont et al. 2001; Hauck et al. 1998; review by Rosenberg et al. 2007; Caldwell et al. 2009). Layers of subhorizontal mica foliations and lineations less abundantly defined by amphiboles manifest a seismic anisotropy inside the near horizontal channel (Guo et al. 2012). Overall geodynamics of the HHSZ may be nearly the same over hundreds of kilometres (Corrie and Kohn 2011). Variations in geometry and orientation of the ramp and the flat along the Himalayan trend have been discussed by Robert et al. (2011a, b) that seem to have no spatial pattern. Based on geochronologic studies of the HHSZ rocks of the Garhwal Himalaya and literature survey, Spencer et al. (2011) concluded that the HHSZ rocks were originally derived from sediments of clastic origin during the late Precambrian along with that from a volcanic arc. Geochemistry of titanites from the HHSZ at Marsyandi section (Nepal) indicate that rocks at a mid-crustal depth were in a partially molten state for ~>10 Ma before the boundaries of the HHSZ were sheared (Kohn and Corrie 2011). Initially, this molten material spread laterally ('tunnelling'), and later, due to monsoonal erosion, it extruded upwards along the HHSZ (Clift et al. 2010; review by Burbank and Anderson 2012). The monsoonal erosion was nonuniform over the HHSZ (Brewer et al. 2006).

The Archean–Proterozoic lithology of the HHSZ (along with few Ordovician granitoids: Lombardo et al. 1993; Carosi et al. 1999) that might be of aluminus composition (Harris 2008) could either be (i) a high-grade metamorphosed equivalent of the Lesser Himalaya or (ii) that of the upper unit of Tethyan Himalaya or even (iii) a mixture of various crustal elements with Greater India due to an early Palaeozoic tectonic event (reviews by Robinson et al. 2006; Chakungal et al. 2010; also Gehrels et al. 2011). Except in the eastern Himalaya, where they are metamorphosed to granulite facies (see Zhang et al. 2010), the HHSZ rocks elsewhere are of greenschist to amphibolite facies (review by Yin 2006).

In the Sutlej section, the HHSZ consists of dominantly schists in the lower part, and gneisses, migmatites and granites in the upper part (Mukherjee and Koyi's 2010a simplification of lithologies). Larson et al. (2010) presented from central Nepal a similar classification of an upper part of the HHSZ with migmatites and kyanite–slilimanite zone rocks and a lower part with garnet–staurolite–kyanite zone (similar review by Wang et al. 2012). A similar classification was also followed by Yakymchuk and Godin (2012) from the far eastern Nepal. These authors identified the contact between the two units both as a metamorphic and a tectonic discontinuity, which could in fact be an out-of-sequence thrust.

In the Annapurna–Manaslu section of the Nepal Himalaya, the HHSZ is divisible into three formations or units—pelitic rocks, calc silicates and augen-gneiss (review by Searle and Godin 2003). Besides, minor amounts of calc silicates, metabasites and retrogressed granulitized eclogites have also been reported from the HHSZ from Sikkim (India) and in parts of Nepal (reviews by Neogi et al. 1998; Carosi et al. 2002, 2007; Rolfo et al. 2008; Gehrels et al. 2011). These rocks of negligible volume will not be considered further in this work.

Inside the HHSZ, an important tectonic unit named as the 'Everest Series' (Searle et al. 2003; Jessup et al. 2008; Streule et al. 2012)/'North Col Formation' (Carosi et al. 1999)/'Chekha Formation' (also spelled as 'Cheka Formation': Kellett et al. 2010; Kellett and Grujic 2012)/'Kumaon Schists' ? (Gansser 1964) has been recognized from different river sections, which consists mainly of calc silicates, marbles and schists with or without high-grade metamorphic minerals, which escaped Cenozoic metamorphism (Carter and Foster 2009). Whereas in the Mt. Everest region in Nepal, it occurs at the structurally topmost part of the HHSZ and did not take part in channel flow (Jessup et al. 2008), in western Bhutan it is present inside the HHSZ as a ~1-km-thick zone. It underwent a top-to-NE sense of ductile shear and presumably was affected by the extrusive flow as a 'coherent unit' (Kellett et al. 2010; also see Tobgay et al. 2012), or its melting

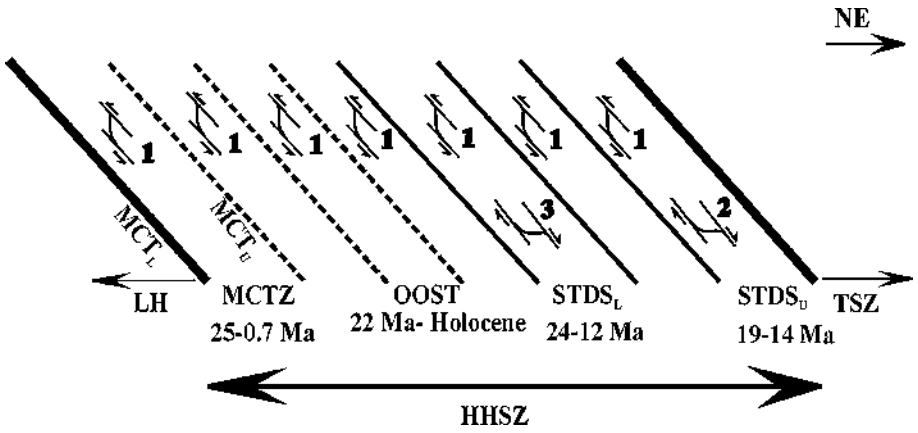

Fig. 3 Summary of the first-order structures on a SW–NE section of the HHSZ. Symbols: '1': top-to-SW shear; '2': top-to-N/NE shear inside the $STDS_U$; '3': that inside the $STDS_L$; HHSZ: Higher Himalayan Shear Zone; TSZ: Tethyan Sedimentary Zone, $STDS_U$: South Tibetan Detachment System-Upper; $STDS_L$: South Tibetan Detachment System-Lower; OOST: out-of-sequence thrust; LH: Lesser Himalaya; MCT_L: Main Central Thrust-Lower, MCT_U Main Central Thrust-Upper; neither to scale nor to dip. Reproduced from fig. 2 of Mukherjee et al. (2012). Timing of activation of the MCT(Z), OOST, $STDS_L$ and the $STDS_U$ are also presented from Godin et al. (2006) and Mukherjee et al. (2012)

contributed to the Higher Himalayan leucogranites/migmatites (Searle et al. 2010).

Throughout the HHSZ, except local folds, the main foliations (and the stretching lineations) dip (and plunge) dominantly towards N/NE. The NW–SE trending HHSZ is bound by the 1 to 10 km-thick 'Main Central Thrust Zone' (MCTZ: reviews by Searle et al. 2003; Godin et al. 2006 and Yin 2006; also see Heim and Gansser 1939; Hubbard and Harrison 1989; Edwards 1995; Gupta et al. 2010; Bell and Sapkota 2012 etc.) in the south as the base and a ductile extensional shear zone: the South Tibetan Detachment System-Upper ($STDS_U$; reviews by Godin et al. 2006; also see Carosi et al. 1998; = 'Inner-South Tibetan Detachment System': Kellett and Godin 2009; Kellett et al. 2010; Kellett and Grujic 2012) in the north within the top (Fig. 3). The MCT_L and/or the MCT_U have been defined based on various tectonometamorphic and geochemical methods (review by Yakymchuk and Godin 2012). Recently, Gray and Pysklywec (2012) proposed based on mathematical modelling of mature continental collision that delamination of the Indian lower crust gave rise to extensional shear near the upper boundary of the HHSZ.

Characterized by mylonitization and bound by the Main Central Thrust-Upper (MCT_U) in the north and the Main Central Thrust-Lower (MCT_L) in the south, the MCTZ could be a tectonic mélange between the Lesser and the Higher Himalayan rocks (reviews by Martin et al. 2005; Godin et al. 2006; and Kohn 2008; Corrie and Kohn 2011; Mottram et al. 2011; Webb et al. 2011). The MCT_L has also alternatively been called as the MCT_1 and the MCT_U as the MCT_2 by many (such as Searle et al. 2008). The MCT(Z) played a crucial role in the Himalayan tectonics, especially after ~25 Ma, by absorbing a significant amount of the India–Eurasia convergence, but possibly the degree of absorption varied along the Himalayan trend (Godard and Burbank 2011; Tobgay et al. 2012). Other than the $STDS_U$ as the upper boundary, a second ductile extensional shear zone—the 'South Tibetan Detachment System-Lower' ($STDS_L$ = Outer-South Tibetan Detachment System: Kellett and Godin 2009; Kellett et al. 2010; Kellett and Grujic 2012)—has been documented inside the HHSZ (Fig. 3) rather discontinuously along the orogenic trend (review and original work by Mukherjee and Koyi 2010a). Along the Himalayan chain, the top-to-S/SW ductile shear of the MCT_L was active between ~15 and 0.7 Ma, the MCT_U at ~25–14 Ma, and the extensional top-to-N/NE ductile shear during ~19–14 Ma within the $STDS_U$ and ~24–12 Ma within the $STDS_L$ (compiled by Godin et al. 2006). Based on available new geochronologic data, Kellett and Grujic (2012) revised the activation span to be 12–11 Ma for the $STDS_U$ in some sections and 22–12 Ma for the $STDS_L$. While the total amount of slip of the $STDS_U$ varies between 42 and 255 km (review by Leloup et al. 2010), for the MCT between 100 and 200 km for the MCT (Johnson and Harley 2010's review), that for the $STDS_L$ has probably remained unconstrained. Unlike the previously held view that the South Tibetan Detachment System developed by continuous deformation of a low-angle normal fault system, it has its genesis linked to both channel flow and extrusion (Kellett and Grujic 2012). Possibly, the MCT_U, the MCT_L and the $STDS_U$ together were active during a brief span of ~15–14 Ma. The exact timing and slip of these tectonic boundaries/zones varied along the entire Himalayan chain. For example, Leloup et al. (2010) deciphered that the extensional shearing inside the $STDS_U$ at the western Himalaya stopped ~5 Ma earlier than in the eastern Himalaya.

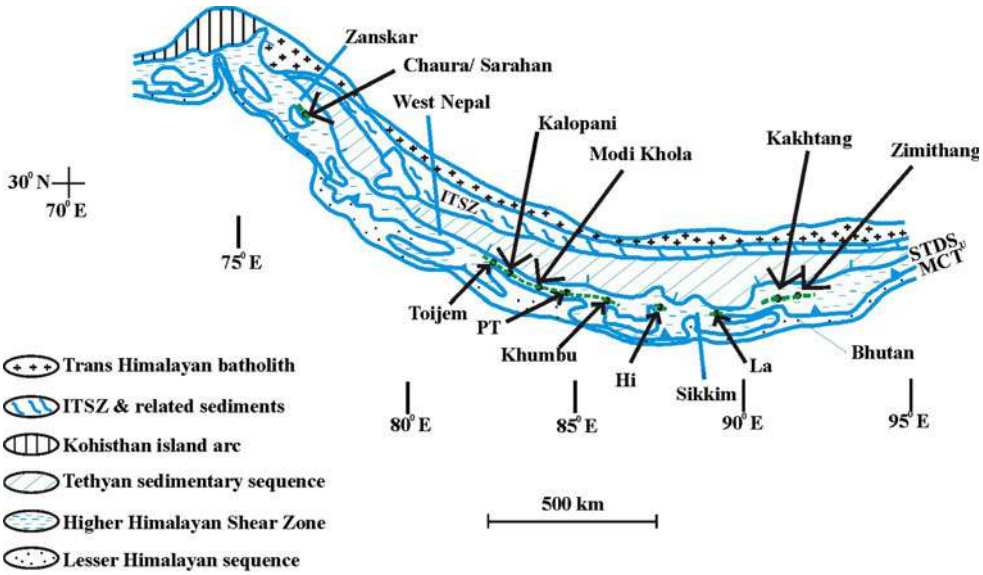

Fig. 4 The out-of-sequence thrust inside the Higher Himalayan Shear Zone (HHSZ). Reproduced from fig. 1 of Mukherjee et al. (2012). The map of the Himalayan chain is reproduced from fig. 1 of Godin et al. (2006). PT: Physiographic Transition; Hi: High Himal Thrust.*Additionally 'La': 'Laya Thrust', plotted from fig. 1b of Warren* et al. *(*2011*), also see* Grujic et al. (2011)

Metamorphism within the HHSZ took place either in two events—in the Eo-Himalayan (>44–33 Ma) and the Neo-Himalayan (~mid-Miocene) periods (reviewed as fig. 7a in Streule et al. 2010), or as a protracted single phase (review by Yakymchuk and Godin 2012). A regional metamorphism during 32–20 Ma up to kyanite to sillimanite grade was reached in the HHSZ (St-Onge et al. 2006). A recent but rather unpopular view has been that the HHSZ underwent a HP metamorphism when it was at a depth of ~80–100 km (Yang et al. 2011). Northward from the MCT_L, an inverted metamorphic gradient gives way northward to a normal sequence of metamorphism (Vannay and Grasemann 2001). Jain et al. (2002) considered a top-to-S/SW ductile shear from ~25 Ma affected the HHSZ. A delay of ~30 Ma in initiating this major phase of deformation starting from the India–Asia collision at ~55 Ma could be due to intensification of erosion rate by the monsoon at ~25 Ma (Clift and Plumb 2008). An out-of-sequence thrust (OOST: Morley 1988's abbreviation) ranging from 22 Ma until Holocene has been deciphered inside the HHSZ based on faster extrusion of its northern part (Fig. 4; review by Mukherjee et al. 2012; in addition, possibly the 'Laya Thrust' in Nepal: Argles 2011; Warren et al. 2011; Grujic et al. 2011). However, Robert et al. (2009) showed that one of these so-called OOSTs—the 'physiographic transitions' in the Nepal Himalaya—is actually a manifestation of overthrusting of a crustal ramp in the subsurface, and therefore should not be considered strictly as OOSTs. Recently, Mukherjee and Bandyopadhyay (2011) documented numerous NE verging backthrusts from the Bhagirathi section of the HHSZ in India.

The geometric and the kinematic parameters—that could be related to extrusion of the HHSZ—varied drastically along the Himalayan trend. For example, (i) the structural thickness of the HHSZ vary from 6 km at the Lower Dolpo in western Nepal (2 km as the lowest thickness of the 'Higher Himalayan Crystallines': Godin et al. 2006; Carosi et al. 2007, 2010; plus 4 km is the thickness of the MCT Zone: Carosi, personal communication) up to 58 km at the Sutlej section (India, Jain and Anand 1988). (ii) Out of eight locations along the Himalayan chain where the thickness of the $STDS_U$ has been reported, the minimum is 350 m in the Annapurna section (Nepal; Searle and Godin 2003), and the maximum is 9400 m in the Sutlej valley (India; Mukherjee and Koyi 2010a) (Fig. 5). (iii) The slip rate of the MCT(Z) at any portion inside it shows a minimum magnitude of 0 mm $year^{-1}$ in the Annapurna section (Nepal, Whipp et al. 2005) and a maximum of 8.4 cm $year^{-1}$ from a portion of Bhutan (Tobgay et al. 2012) (Fig. 6). (iv) Likewise, the slip rate of the $STDS_U$ varies from 0.7 mm $year^{-1}$ in the Sutlej section (India, Vannay et al. 2004) up to 47 mm $year^{-1}$ at Mansalu area (Nepal, Hodges et al. 1998) (Fig. 6). (v) During its genesis, the proto-HHSZ had a maximum slope of 60° at ~24 Ma (fig. 2 of Jamieson et al. 2004). With time, as the HHSZ extruded towards S/SW, it developed a gentle dip of 30° (fig. 2b of Vannay and Grasemann 2001) or 40° (fig. 6 of Yin 2006; also see Carosi et al. 2010). However, in rare cases, a steeper dip of 60° still persists at places in the central Himalaya (Yin 2006). (vi) Ten magnitudes of pressure gradients available at eight locations reveal a minimum of ~0.02 kb km^{-1} east to La Kang valley (Bhutan, Grujic et al. 1996) and a maximum of 6 kb km^{-1} in the Langtang section (Nepal, Kohn 2008) (Fig. 7). Some of these parameters are the metamorphic pressure gradient, which could be correlated tentatively with lithostatic/tectonic pressure gradient (review by Huetra et al. 1999; Larson

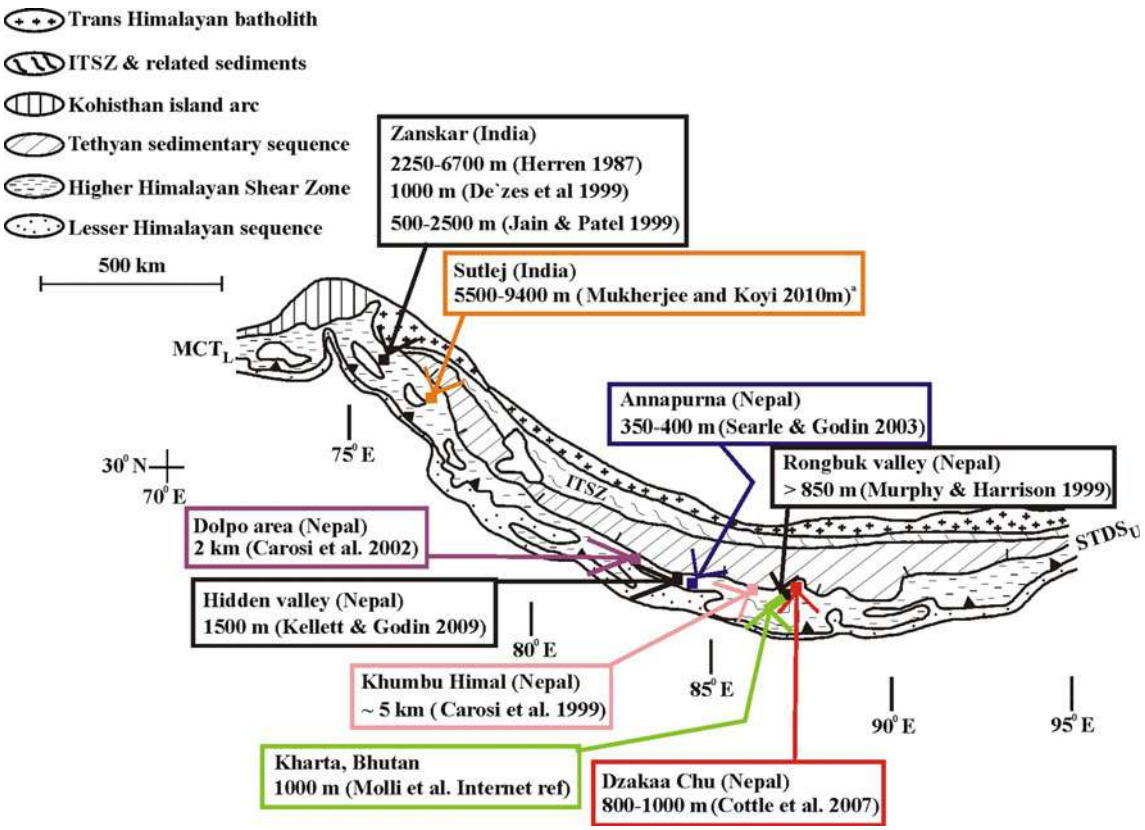

Fig. 5 Thickness of the South Tibetan Detachment System-Upper ($STDS_U$) reported from different sections of the Higher Himalayan Shear Zone compiled from previous authors. The map of the Himalayan chain is reproduced from fig. 1 of Godin et al. (2006)

et al. 2010). (vii) A component of pure shear was invoked to account for the presence of either shear bands or flattened folds in the HHSZ found at least at four locations (Bhattacharya 1999; Goscombe et al. 2006; Cottle et al. 2007; Mukherjee 2007, 2010a; Mukherjee and Koyi 2010a) along the Himalayan trend. In addition, the kinematic vorticity number (W_k: 'a nonlinear ratio between simple shear to pure shear deformation': Johnson et al. 2009) has been constrained within nine ranges at five different locations. The W_k values vary from 0.57 (i.e. more of pure shear component than simple shear) up to 0.85 (=more of simple shear component than pure shear; Rongbuk section, Nepal, Jessup et al. 2006) (Fig. 8). All these magnitudes of pressure gradients, strain rates and rates of slip (Figs. 5, 6, 7, 8) hold true only for different shorter time intervals that fall within 0–25 Ma. The displacement (slip) across the $STDS_U$ was >50 km (Burchfiel et al. 1992) and the MCT was 200–210 km (reviews by Johnson 2002; Yin 2006)—but these data were not utilized in the present model.

(viii) Bound at south by (meta/)sediments of Lesser Himalaya and at north by the Tethyan Himalaya (Fig. 3) of much lesser thermal conductivity (Grasemann 1993), the HHSZ releases considerable heat (4–5 $\mu W\ m^{-3}$: at Sikkim, India: Faccenda et al. 2008). The Dalhousie group of researchers in their coupled thermal mechanical model implicitly assumed a geothermal gradient of 18–28 °C km^{-1} for the HHSZ (as estimated by Spencer et al. 2012). Out of merely seven locations where the geothermal gradient has been constrained, an anomalously low magnitude of 5.5 °C km^{-1} was reported from Sikkim (India, Neogi et al. 1998) and a high apparent thermal gradient of 420 °C km^{-1} during Miocene Period from the Sutlej section (Francsis 2012) (Fig. 9). From three known magnitudes, the HHSZ rocks vary in thermal conductivity from 1.5 W m^{-1} K^{-1} at Garhwal (India, Ray et al. 2007) up to a maximum of 5.3 W m^{-1} K^{-1} at the Marsyandi basin (Nepal, Annen et al. 2006) (Fig. 9), which is ~1.5 times greater than the average value of ~3.45 W m^{-1} K^{-1} for the average conductivity value for the Indian subcontinental crust (as referred by Sarkar and Saha 2006; Maj 2008). In general, for a channel flow to occur in rocks that are a partially molten, a high heat production of ≥c. 2 mW m^{-3} is expected (Kohn and Corrie 2011). Viscous dissipation due to ductile shear in the HHSZ must have varied significantly along the orogenic trend (Mukherjee 2012b).

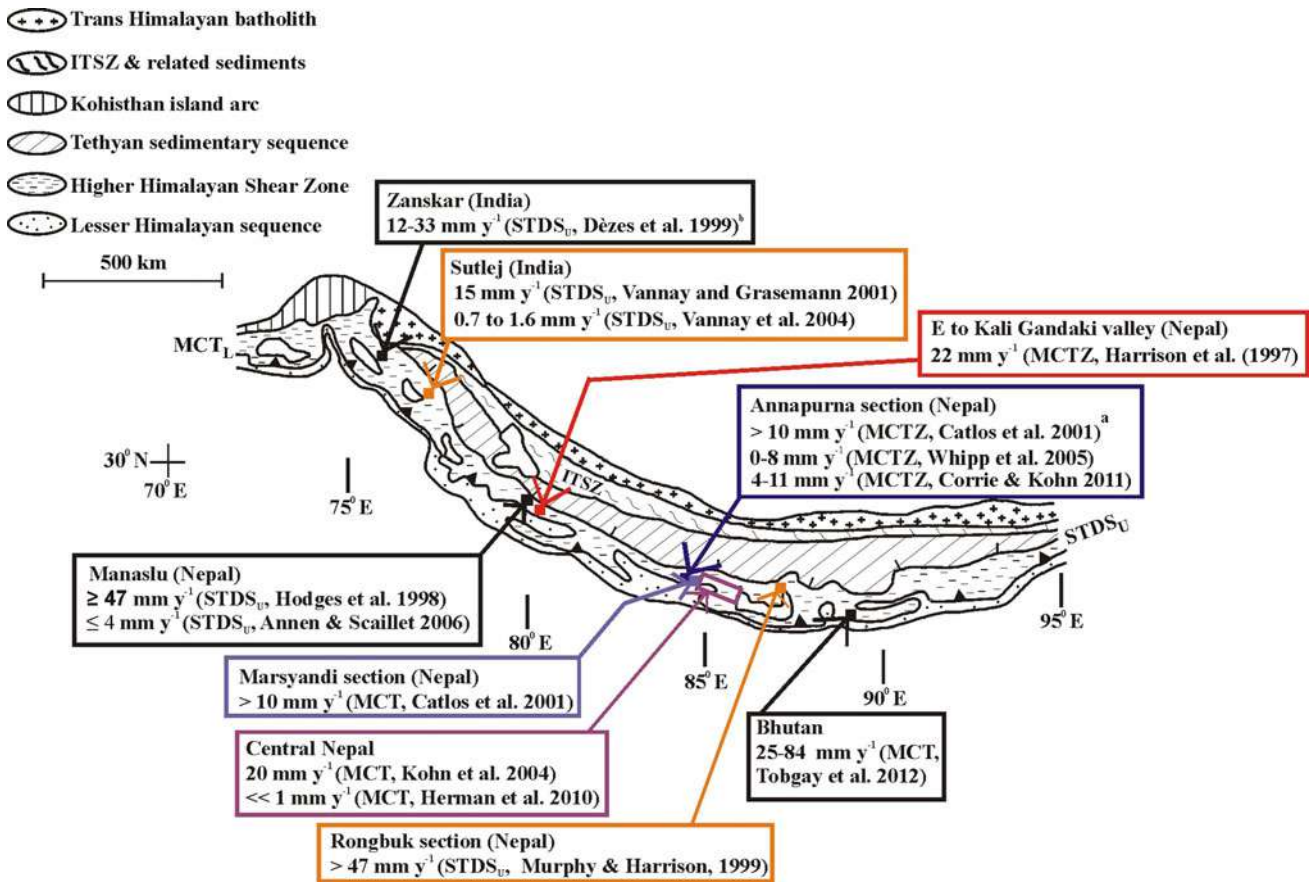

Fig. 6 Slip rates of the Main Central Thrust Zone (MCTZ) and the South Tibetan Detachment System-Upper ($STDS_U$) estimated for the Higher Himalayan Shear Zone compiled from previous authors. **a**, **b** As referred in Vannay and Grasemann (2001). **c**, **d** *Exhumation rate of the MCT(Z) of the authors is written as slip rate in this work.* The map of the Himalayan chain is reproduced from fig. 1 of Godin et al. (2006)

An analytical model

A channel with very long and rigid parallel inclined boundaries is considered to be filled with an incompressible Newtonian fluid. The coordinate axes are chosen such that the positive side of the *Z*-axis is along the up-dip direction (Fig. 10). A '*component of gravity*', expressed as the product of density, acceleration due to gravity and the sine of the dip of the shear zone, tends to subduct the fluid (Eqs. 1 and 2 in the 'Appendix 2'). A component of pressure gradient tends to counteract the 'component of gravity' and extrude the fluid. The 'Poisson equation' of flow (Eq. 1 in 'Appendix 2') is solved to obtain the velocity profile (see Beaumont and Ings 2012, Natarov and Conrad 2012 etc. for alternate but effectively the same expressions). The channel is now equated with the HHSZ with an N/NE dip direction. The model considers that deformation and extrusion of the HHSZ is governed by (i) slip of its boundaries; (ii) a pressure gradient; and (iii) a gravity component. What has been reported as 'pressure gradient' in the literature (reviewed in Fig. 7) must be the '*resultant pressure gradient*' (='$\partial P/\partial z - d\ g\ \mathrm{Sin}\theta$' in Eq. 1 in 'Appendix 2'), which is the component of pressure gradient minus the gravity component. It is certainly not the '$\partial P/\partial z$' of equation in 'Appendix 2', as in that case, ($\partial P/\partial z - d\ g\ \mathrm{Sin}\theta$) becomes less than zero leading to subduction and no extrusion at all.

Across the vertex (Fig. 10), opposite shear senses develop simultaneously within the two subzones. Under a certain algebraic relation among the flow parameters, the vertex lies inside the shear zone (in Eq. 4 in 'Appendix 2'), and the parabolic profile tapers towards the up-dip direction. In the context of the HHSZ, the reverse shear subzone formed at the upper portion equates with the $STDS_U$ with a top-to-N/NE sense of ductile shear. The location of the vertex depends on the following flow parameters: (i) the absolute velocities of the two boundaries; (ii) thickness of the shear zone; (iii) *resultant* pressure gradient along the shear zone; and (iv) viscosity of the rock (expressions between Eqs. 3 and 4 in 'Appendix 2'). The resultant pressure gradient is in turn dependent on (iiia) the pressure

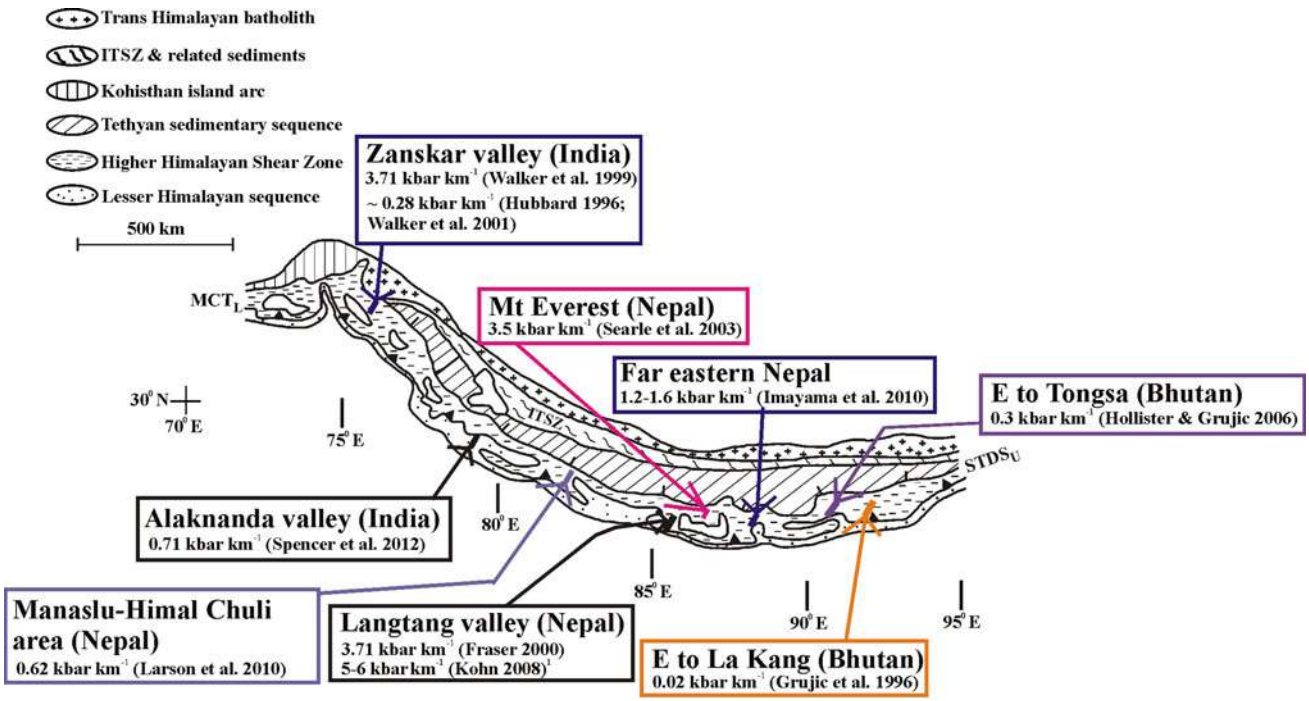

Fig. 7 Pressure gradient estimated for the Higher Himalayan Shear Zone (HHSZ). Data by previous authors have been compiled. The map of the Himalayan chain is reproduced from fig. 1 of Godin et al. (2006)

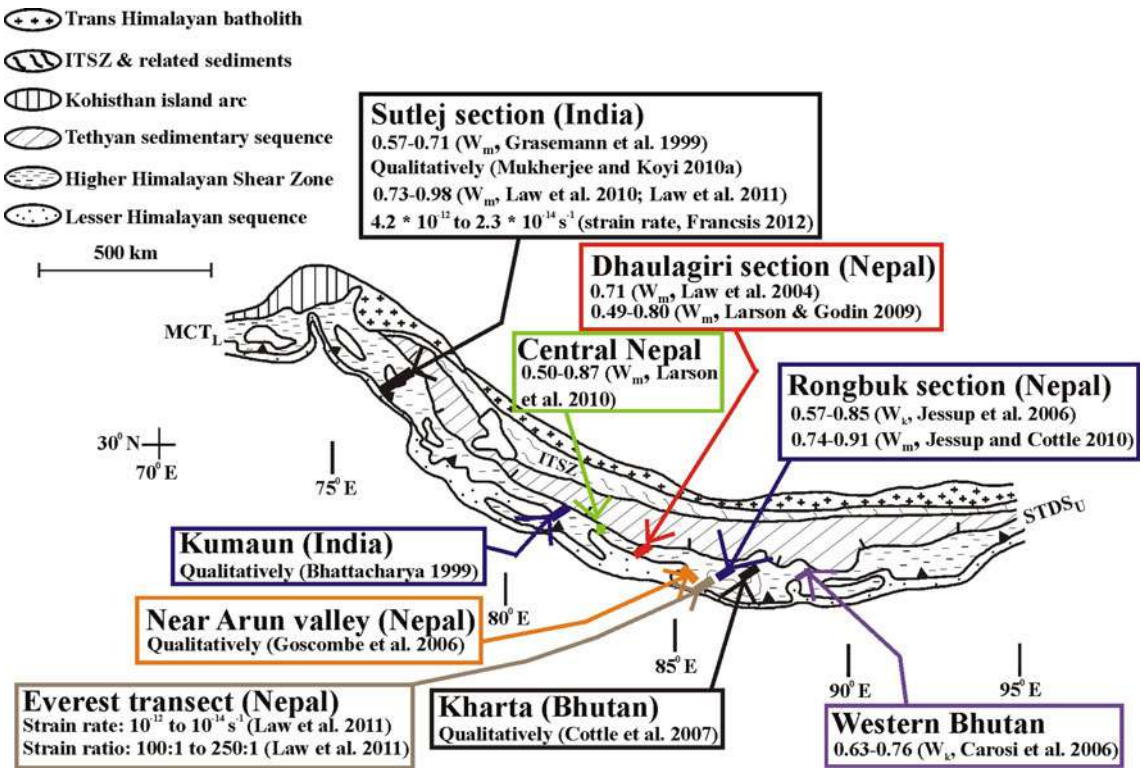

Fig. 8 The 'kinematic vorticity number' (W_k) and the 'mean kinematic vorticity number' (W_m) estimated for the Higher Himalayan Shear Zone compiled from previous authors. In few cases, pure shear was deciphered qualitatively based on the presence of shear bands and are *indicated by 'qualitatively'*. The 'strain ratio' is the ratio between the minimum to the maximum stretch (Park 1997). The map of the Himalayan chain is reproduced from fig. 1 of Godin et al. (2006)

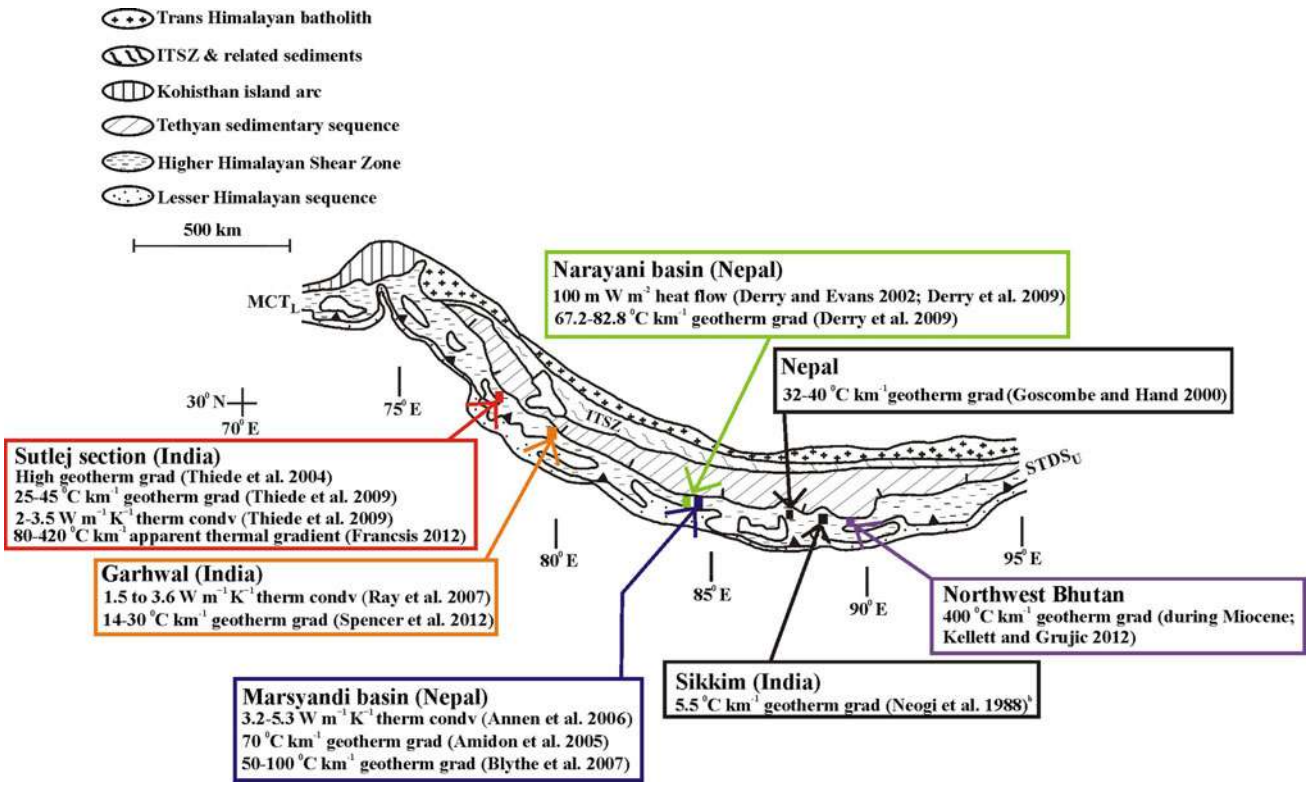

Fig. 9 Thermal parameters for the Higher Himalayan Shear Zone compiled from previous authors. The map of the Himalayan chain is from fig. 1 of Godin et al. (2006)

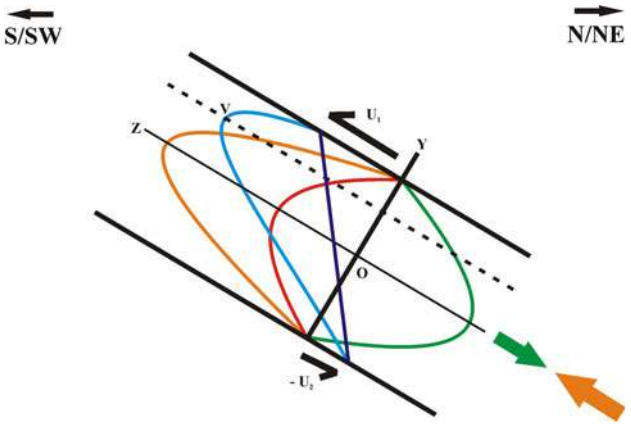

Fig. 10 Extrusion of the Higher Himalayan Shear Zone (HHSZ) by means of a channel flow mechanism shown in a cross-section along N/NE–S/SW geographic directions. A combination of simple shear at the boundaries (*half arrows*) and a resultant pressure gradient that drives rock upwards is represented. *Green* profile: gravity-induced flow. *Orange* profile: a flow component that tries to extrude. *Red* profile: the resultant of the previous two profiles. *Blue* profile: the grand resultant profile between simple shear and the *red* profile. Sizes of the two *full arrows*: rigour of the respective flows given by their colours. V: Vertex, through which a dash line parallel to the boundaries represent the lower boundary of reverse ductile shear

gradient that pushes the rock upward; (iiib) dip of the shear zone; (iiic) acceleration due to gravity; and (iiid) density of the rock (Eq. 1 in 'Appendix 2').

Notice that (i) the location of the vertex and the flow equation from which it was derived (expressions between Eqs. 3 and 4 in 'Appendix 2') are independent of total time taken for channel flow extrusion (no 't' term exists in Eq. 1 in 'Appendix 2') and the extrusion rate of the shear zone; (ii) as in Grujic et al. (1996, 2002) and Mukherjee and Koyi (2010a), kinematic vorticity numbers and erosion rates were *not* incorporated in the flow equation; (iii) the thickness of the MCT Zone is absent in the flow equation; and (iv) the dip of the HHSZ does appear in the flow equation ('θ' in Eq. 1 in 'Appendix 2'), unlike the model horizontal channels by Mukherjee and Koyi (2010a, b). However, since along with other magnitudes, that for the 'resultant pressure gradients' ('$\partial P/\partial z - d\ g\ \mathrm{Sin}\theta$' in Eq. 1 in 'Appendix 2') were inserted to estimate the viscosity (Table 1), the magnitudes of dip did not find any direct use. Field-studies on the HHSZ can delineate the $STDS_U$, and hence estimate its thickness. The other parameters such as lithostatic pressure gradient comes from metamorphic studies (e.g. Neogi et al. 1998) and the slip rate of the boundaries from geochronology (such as Catlos et al. 2001). Application of a single model to different sections of the Higher Himalaya is certainly a simplification where the second order tectonic features of individual sections had to be ignored.

Table 1 Rows 1–14: a few flow parameters of 'solid' and partially molten rocks, and Earth's segments (crust, lithosphere, etc.) collected from theliterature

Sl no	Lithology	Density (d; in gm cm^{-3})	Thermal diffusivity (κ; in m s^{-2})	Viscosity (in Pa s)	Prandtl number (P_r; no unit)
1	Limestone	1.6[a]–2.84[b]	1.1×10^{-6} [a]	10^{17}–10^{21} [a]	3.2×10^{19}–5.2×10^{23}
2	Granite	2.5[c]–2.8[c]	0.6×10^{-6} [b]–2.1×10^{-6} [c]	10^{3} [b] (at 1400 °C); 10^{20} [c] (at near surface)	5.1×10^{7}–2.8×10^{22}
3	Schist	2.4[a]–2.9[a]	1.3×10^{-6} [c]–1.8×10^{-6} [c]	10^{18} [d] –10^{19} [d] (500–700 °C)	2.8×10^{20}–3.5×10^{21}
4	Gneiss	2.59[d]–3.12[e]	1.2×10^{-6} [a]	8×10^{18} [e]–0.3×10^{23} [f]	2.7×10^{23}–3.2×10^{26}
5	Granulite	3.1[f]	0.65×10^{-6} [d]–1.4×10^{-6} [e]	10^{19} [g]	7.1×10^{23}–1.5×10^{24}
6	Migmatite	~2.8 [g]–3.1[g]	0.8×10^{-6} [f], 1.2×10^{-6} [g]	10^{16} [h]–10^{20} [h]	2.7×10^{18}–4.5×10^{22}
7	Most magmas	2.2 [h]–3.1[h]			
8	Partially molten rock (in low viscosity channel at a mid-crustal depth)	2.4[i]–2.9[i]	0.5×10^{-6} [h]	10^{18} [i]–10^{19} [i]	8.3×10^{20}–6.9×10^{21}
9	Average igneous rocks		0.12×10^{-6} [i]		
10	Continental crust	2.7[j]–2.9[k]	~0.6×10^{-6} [j]–1×10^{-6} [k]	6×10^{18} [j]–10^{21} [j]	2.1×10^{21}–6.1×10^{23}
11	Lithosphere		~0.6×10^{-6} [j]–1×10^{-6} [k]	10^{21} [k]–10^{23} [k]	
12	Strong mantle lithosphere (superstructure)			10^{22} [l]–10^{24} [l]	
13	Weak mantle lithosphere (infrastructure)			10^{19} [m]–10^{20} [m]	
	Tso Morari Gneiss dome	2.59[d]–3.12[e]	1.2×10^{-6} [l]	$\leq 8 \times 10^{22}$ [n]	$\leq 5.6 \times 10^{28}$ [a]
14	The entire Earth	5.5[l]	0.36×10^{-6} [m]–0.36×10^{-7} [n]	2×10^{19} [o]	10^{22}–10^{23} [b]
15	Higher Himalayan Shear Zone (HHSZ) along the studied Himalayan trend	2.2 [m]–3.1[n]	0.5×10^{-6} [o]–2.1×10^{-6} [p]	10^{16}–10^{23} (this work)	10^{21}–10^{28} (this work)
16	Higher Himalayan Shear Zone (HHSZ) in Sutlej section	2.2[o]–3.1[p]	0.5×10^{-6} [o]–2.1×10^{-6} [p]	10^{17}–10^{23} (this work)	10^{22}–10^{28} (this work)

Rows 16: chosen ranges of density and thermal diffusivity of the Higher Himalayan Shear Zone (HHSZ) and its estimated viscosity and Prandtl number

References: *Density column:* a. Turcotte and Schubert (2002); b. Mizutani (1984); c. Henderson and Henderson (2009); d. Landholt-Bornstein (1982); e. Carmichael (1989); f. Boyd and Meyer (1979); g. Michael Brown (personal communication); h. Mcbirney (1994); i. Zhu et al. (2010); j. Ernst and Liou (2008); k. McCall (2005). l. Turcotte and Schubert (2002); m to p. These values are the highest and the lowest densities of the constituent rocks of the HHSZ except limestones. *Thermal diffusivity column:* a. Buntebarth (1984); b. Heuze (1983); c. Whittington et al. (2009); d. Kukkonen et al. (1999); e. Ray et al. (2006); f. Tanner (1999); g. Thompson (1999); h. taken from Whittington et al. (2009); i. Stacey (1969); j. Bott (1971); k. Davies (2001), Fowler (2005), Philpotts and Ague (2009); l. Data of Davies (1980) as used by Mukherjee and Mulchrone (2012); m, n: these are calculated from rest of the data for the entire Earth; o, p: these values are the minimum and the maximum magnitudes of thermal viscosities among that of all the constituent lithologies. *Viscosity column:* a. Review and original data by Gunzburger (2010); also data used in models by Stein and Wickham (1980). b. Petford et al. (2000); c, d. Davidson et al. (1994). e. Beaumont et al. (2009); f. Dong (2002); g. Gerya et al. (2000), Perchuk and Gerya (2011); h. Review by Barraud et al. (2004); i. Zhu et al. (2010); j. value of lower crust below the Tibetan plateau—Harris (2007); k. Dennis (1987); l. Tolkunova (1977), Watts (2001); Fowler (2005), etc.; m. Review by Harris (2007); n. Mukherjee and Mulchrone (2012); o. Scheidegger (1982a, b). *Prandtl number Column*: a. Mukherjee and Mulchrone (2012); b. Davies (1980)

Note: (i) The range of Prandtl number (P_r) is calculated based on $(P_r)_{max} = \mu_{max}\, d_{min}^{-1}\, \kappa_{min}^{-1}$ and $(P_r)_{min} = \mu_{min}\, d_{max}^{-1}\, \kappa_{max}^{-1}$; where μ, dynamic viscosity; d, density; κ, thermal diffusivity. (ii) Spaces in the tables that are vacant are the parameters that were either not used in this work (e.g. density of the lithosphere) or were not available in the literature (density of the superstructure and the infrastructure)

Not all the flow parameters are available for any individual section across the Higher Himalaya. For example, in the Sutlej section of the HHSZ, (i) the slip rate of the MCTZ and (ii) the resultant pressure gradient are unavailable (compare Figs. 5, 6, 7, 8). Taking the maximum and minimum values of slip of the MCT(/Z) from other Himalayan sections (i.e. 0 mm year^{-1} from Annapurna section, Nepal: Whipp et al. 2005; and 8.6 cm year^{-1} in Bhutan: Tobgay et al. 2012) and those for the $STDS_U$ from the Sutlej section itself (i.e. 0.7–1.6 mm year^{-1}: Vannay et al. 2004), the approximate minimum and the maximum total slip rates (the '$U_1 + U_2$' in Eq. 7 in 'Appendix 2') for the Sutlej section of the HHSZ are calculated to be 0.7 and 87.6 mm year^{-1}, respectively. That the minimum slip rate for the absolute movement of the MCTZ in the Sutlej section could be very low is supported by the presence of an out-of-sequence thrust (OOST; review by Mukherjee et al. 2012). This is because Herman et al.'s (2010) tectonic modelling demonstrated that for an OOST to occur inside the HHSZ, the slip rate in the MCTZ needs to be $\ll$1 mm year^{-1}. The two extreme values of pressure gradient were considered from some other sections, for example 0.02 kbar km^{-1} from east to La Kang (Bhutan, Grujic et al. 1996) and 6 kbar km^{-1} from Langtang valley (Nepal, Kohn 2008) (Fig. 7). Using figs. 1 and 3 of Mukherjee and Koyi (2010a), the thickness of the Sutlej section of the HHSZ and those of the $STDS_U$ were found to be $\sim$58 and $\sim$9.4 km when the HHSZ is considered to have a 60° dip, and 34 and 5.5 km when the dip is 30°.

A comparison between the data obtained for the Sutlej section and those from all other sections can now be made. The highest known thickness of 9.4 km of the $STDS_U$ comes from the Sutlej section (Fig. 5; Mukherjee and Koyi 2010a). The slip rate of the $STDS_U$ of 0.7–15 mm year^{-1} (Vannay and Grasemann 2001; Vannay et al. 2004) is much below the maximum known rate of 47 mm year^{-1} from the Manaslu section (Nepal; Hodges et al. 1998; see Fig. 6). The highest mean kinematic vorticity number ($W_m = 0.98$: Law et al. 2011) in the HHSZ has been deduced from the Sutlej section. The highest geothermal gradient of 45 °C km^{-1} (Thiede et al. 2009) and a highest apparent thermal gradient of 420 °C km^{-1} (Francsis 2012) were also deciphered from this section. Likewise, the maximum thermal conductivity of the HHSZ rocks at this section of 3.5 W m^{-1} K^{-1} (Thiede et al. 2009) is less than the deciphered maximum magnitude of 5.3 W m^{-1} K^{-1} from the Marsyandi section (Annen et al. 2006).

A review on density (d), thermal diffusivity (κ) and dynamic viscosity (μ) of the five types of rocks—schists, gneisses, migmatites, granites and granulites of the HHSZ (second to sixth rows in Table 1)—reveal that those parameters for all these rocks taken together range between d: 2.2–3.1 gm cm^{-3}, κ: 0.6×10^{-6}–2.1×10^{-6} m s^{-2}, and μ: 10^3–10^{21} Pa s. Calculation of Prandtl number (P_r) of these rocks using the formula $P_r = \mu\ d^{-1}\ \kappa^{-1}$ gives a range of magnitudes for all these rocks from $\sim 5.1 \times 10^7$ to $\sim 1.5 \times 10^{24}$ (sixth column in Table 1). These ranges of 'd' and 'κ' were taken for the HHSZ to estimate its viscosity and Prandtl number (rows 15 and 16 in Table 1). Thus, in this process of calculation, the set of magnitudes chosen to estimate viscosity and Prandtl number may not match with any single rock type (compare rows 1–14 with 15–16 in Table 1). The final set of parameters and their ranges of magnitudes used to estimate the viscosity and the Prandtl number are shown in Table 2. Various possible ranges of values taken in this study are shown in Table 3. Notice that the calculation of viscosity is not possible if the thickness of the $STDS_U$ (=9.4 km) is considered to be more than that of the HHSZ (=4 km). The $STDS_U$ being a zone inside the HHSZ, the former must be considered thinner than the latter.

Now consider magnitudes for parameters related to extrusion of the HHSZ along the trend of the Himalaya that is not specific to any section. Since the slip rate of the MCT along the Himalayan trend vary between 0 and 8.4 cm year^{-1} and that of the $STDS_U$ between 0.7 and 47 mm year^{-1} (Fig. 6), the total slip rate of these two units along the Himalaya ranges from 0.7 to 131 mm year^{-1} ($0 + 0.7 = 0.7$; $84 + 47 = 131$). The thickness of the $STDS_U$ was taken to vary from 0.35 km (data at Annapurna section, Nepal: Searle and Godin 2003) to 9.4 km (at Sutlej section, India: Mukherjee and Koyi 2010a), and that of the HHSZ from 6 (Lower Dolpo, Nepal: Carosi et al. 2007, Carosi et al. 2010) up to 58 km (Sutlej valley, India: Jain and Anand 1988). The ranges of magnitudes for the pressure gradient (0.02–6 kb km^{-1}), dip (30–60°), density (2.2–3.1 gm cm^{-3}) and thermal diffusivity (0.5×10^{-6}–2.1×10^{-6} m s^{-2}) of the HHSZ (compiled in Table 4) are same as the case considered for the Sutlej section. Thermal

Table 2 The maximum and the minimum magnitudes of parameters to estimate the viscosity and Prandtl number of the Sutlej section of the Higher Himalayan Shear Zone (HHSZ)

Slip rate ($U_1 + U_2$) in mm year^{-1}	Thickness of HHSZ ($2y_0$) in km	Resultant pressure gradient ($\partial P/\partial z - d\ g\ \mathrm{Sin}\theta$) in kbar km^{-1}	Density of HHSZ (d) in gm cm^{-3}	Thickness of the $STDS_U$ (T) in km	Thermal diffusivity (κ) in m s^{-2}
0.7	34	0.02	2.2	5.5	0.5×10^{-6}
87.6	58	6	3.1	9.4	2.1×10^{-6}

Table 3 Calculation of viscosity 'μ' of the Higher Himalayan Shear Zone (HHSZ) in the Sutlej section

Sl no	Slip rate ($U_1 + U_2$) in mm year^{-1}	Thickness of HHSZ ($2y_0$) in km	Resultant pressure gradient ($\partial P/\partial z - d\ g\ \mathrm{Sin}\theta$) in kbar km^{-1}	Thickness of the $\mathrm{STDS_U}$ (T) in km	Viscosity of HHSZ (μ) in Pa s
1	87.6	34	0.02	5.5	2.6×10^{20}
2	87.6	34	6	5.5	**8.7×10^{17}**
3	87.6	58	0.02	9.4	7.5×10^{20}
4	87.6	58	6	9.4	2.5×10^{18}
5	0.7	34	0.02	5.5	3.8×10^{21}
6	0.7	34	6	5.5	3×10^{19}
7	0.7	58	0.02	9.4	**1.3×10^{23}**
8	0.7	58	6	9.4	8.5×10^{19}

The maximum (1.3×10^{23} Pa s) and the minimum estimates (8.7×10^{17} Pa s) are shown in bold

Table 4 The maximum and the minimum magnitudes of parameters used to estimate the viscosity and Prandtl number of the Higher Himalayan Shear Zone (HHSZ) along the studied Himalayan trend

Slip rate ($U_1 + U_2$) in mm year^{-1}	Thickness of HHSZ ($2y_0$) in km	Resultant pressure gradient ($\partial P/\partial z - d\ g\ \mathrm{Sin}\theta$) in kbar km^{-1}	Density of HHSZ (d) in gm cm^{-3}	Thickness of the $\mathrm{STDS_U}$ (T) in km	Thermal diffusivity (κ) in m s^{-2}
0.7	6	0.02	2.2	0.35	0.5×10^{-6}
131	58	6	3.1	9.4	2.1×10^{-6}

Table 5 Calculation of viscosity 'μ' of the Higher Himalayan Shear Zone (HHSZ) along the studied Himalayan trend

Sl no	Slip rate ($U_1 + U_2$) in mm year^{-1}	Thickness of HHSZ ($2y_0$) in km	Resultant pressure gradient ($\partial P/\partial z - d\ g\ \mathrm{Sin}\theta$) in kbar km^{-1}	Thickness of the $\mathrm{STDS_U}$ (T) in km	Viscosity of HHSZ (μ) in Pa s
1	0.7	6	0.02	0.35	3.7×10^{20}
2	0.7	6	6	0.35	2.7×10^{19}
3	0.7	58	0.02	0.35	3.2×10^{17}
4	0.7	58	6	0.35	1.1×10^{20}
5	131	58	0.02	0.35	3.3×10^{20}
6	131	58	6	0.35	1.1×10^{18}
7	131	6	0.02	0.35	3.6×10^{18}
8	131	6	6	0.35	**1.2×10^{16}**
9	131	58	0.02	9.4	**1.3×10^{23}**
10	131	58	6	9.4	3.6×10^{20}
11	131	58	0.02	9.4	2.1×10^{20}
12	131	58	6	9.4	4.2×10^{18}

The maximum (1.3×10^{23} Pa s) and the minimum estimates (1.2×10^{16} Pa s) are shown in bold

diffusivity can vary with depth (Nabelek et al. 2010) and with temperature (Nabelek et al. 2012), but for the sake of simplicity, this variation is not considered in this work. A number of combination of magnitudes to estimate viscosity and Prandtl number are shown in Table 5.

The estimated range of viscosities of the HHSZ (and not of its constituent individual rock types) along the studied Himalayan trend comes out to be $\sim 10^{16}$–10^{23} Pa s (row 15 in Table 1) and that for only the Sutlej section within $\sim 10^{17}$–10^{23} Pa s (row 16 in Table 1). The ranges of Prandtl numbers in these two cases are estimated to be $\sim 10^{21}$–10^{28} and $\sim 10^{22}$–10^{28}, respectively. As expected, the calculated ranges of viscosity and Prandtl number for the Sutlej section of the HHSZ falls within the respective ranges for the HHSZ along the Himalayan trend.

Discussions

Whereas the ramp-flat geometry of the HHSZ might vary along the Himalayan chain (Robert et al. 2011a, b), the ramp alone defines the model channel through which

extrusive flow is defined. The present approach of modelling ductile deformation in terms of boundary conditions and rheology of the shear zone is similar to those adopted by many previous workers (e.g. Beaumont et al. 2001; Grujic et al. 1996, 2002; Ramsay and Lisle 2000; Stüwe 2007; Mancktelow 2008). However, any possible temporal variation in the amount and the rate of extrusion of the HHSZ (Kellett et al. 2010) vis-à-vis its rheologic heterogeneity are not considered in the flow model (Eq. 1 in 'Appendix 2'). Also not considered are the pre-Himalayan D_1, and the post-Himalayan D_3 and the D_4 deformations (of Jain et al. 2002) that gave rise to folding and brittle faulting. Rather, the model considers only the Himalayan D_2 deformation phase when a top-to-SW ductile shear sense developed inside the HHSZ along with a channel flow.

The viscosity ranges deduced in this work falls well within 10^{17}–10^{25} Pa s of all the rock types as referred by Gerya and Meilick (2011). The viscosities and Prandtl numbers estimated for the HHSZ in two cases have rather wider ranges since the input parameters such as pressure gradient, thickness of the HHSZ and that of the $STDS_U$, and the total slip rates of the MCT and the $STDS_U$ themselves vary widely in magnitudes. By contrast, since the density (d: 2.2–3.1 gm cm^{-3}) and the thermal diffusivity (κ: 0.5×10^{-6}–2.1×10^{-6} m s^{-2}) of the HHSZ were considered to vary within much narrower limits, they were not responsible for yielding those wide ranges.

As calculated for the Sutlej section here, using specific magnitudes of parameters for any particular section of the HHSZ, one can estimate viscosity and Prandtl number of the HHSZ at that transect. The range of viscosity deduced for the HHSZ of Sutlej section has a little tighter range of 10^6 than that of 10^7 as estimated for the HHSZ along the complete Himalayan trend. This is because while the maximum total slip rate (the '$U_1 + U_2$' in Eq. 7 in 'Appendix 2') for the HHSZ along the Himalayan trend is 131 mm year^{-1} (as entered in first column in Table 4), that for the Sutlej section is merely 87.6 mm year^{-1} (in Table 2). Since the same range of density (d: 2.2–3.1 gm cm^{-3}) and thermal diffusivity (κ: 0.5×10^{-6}–2.1×10^{-6} m s^{-2}) were considered to estimate the Prandtl number in both the cases, the range calculated for the Sutlej section was narrower than that for the complete HHSZ. Significantly narrowing the estimates of the pressure gradient, the thicknesses of the HHSZ and $STDS_U$ and the slip rates of the MCT and the $STDS_U$ in any section would significantly shorten the calculated range of viscosity and Prandtl number for that section. The upper limit of viscosity of the HHSZ of $\sim 10^{23}$ Pa s matches with the high magnitude as predicted by Copley et al. (2011) beneath Tibet. The Tibetan middle crust extruded from a subhorizontal channel that was connected with the inclined HHSZ. However, whereas Copley et al. (2011) concluded that such a high viscosity cannot favour a channel flow, the present work inputs the existing extrusion parameters into the flow equation to reach the high magnitude as one of the possibilities. Based on the experimental rock mechanical data, Rutter et al. (2011) estimated the viscosity of the Tibetan mid-crust to range widely between 10^{15} and 10^{21} Pa s. On the other hand, 3D mechanical modelling along with GPS studies led He et al. (2012) to reach a tighter range of 10^{19}–10^{23} Pa s for the lower crust of the Tibetan plateau. Thus, keeping in mind the uncertainties in estimating viscosity in the present work, the deduced viscosity range of the HHSZ broadly conforms with the recent findings (Copley et al. 2011; Rutter et al. 2011; He et al. 2012) for the mid- to lower crustal materials of Tibet.

The estimated variation in viscosity of the HHSZ in two cases nearly encompasses the magnitudes for its constituent rocks, viz. schists, migmatites and granulites (compare rows 2–6 with 15–16 in Table 1). However, the lower limit for hot molten granites ($\sim 10^3$ Pa s) falls far outside the deduced ranges for the HHSZ. This was anticipated since as the HHSZ also includes schists of higher viscosity. The representative viscosity of the HHSZ is expected to be higher than that of a pure granitic melt. The volume of granitic melt produced along the Himalayan chain might have varied. Similarly, while the ranges for the HHSZ cover those for the Earth, the continental crust and the 'weak mantle lithosphere (infrastructure)', it partly matches with the 'strong mantle lithosphere (superstructure)' and partly with the 'weak mantle lithosphere (infrastructure)' (compare rows 10–14 with 15–16 in Table 1). As partially molten rocks at 'mid-crustal depth' were a significant contributor for the channel flow extrusion of the HHSZ, it is expected to be mechanically weak and presumably similar to an infrastructure.

The estimated range of Prandtl number ($\sim 10^{21}$ to $\sim 10^{28}$) for the HHSZ embraces those for schists, migmatites, granulites, continental crust and the entire Earth, but greatly exceeds the lower limit for the granite melts ($\sim 10^7$), for magmas in general ($\sim 10^4$–10^8: Lappa 2010), and the highest limit exceeds that for mantle ($>10^{20}$ to $\sim 10^{24}$: Jarvis and Peltier 1989; Olson 1989; Matyska and Yuen 2007; Lappa 2010 etc.) by five orders of magnitudes or so. Note that the upper limit of Prandtl numbers of the HHSZ nearly equals that estimated for the Tso Morari gneiss ($\sim 10^{28}$: Mukherjee 2011d; Mukherjee and Mulchrone 2012). A relatively faster rate of heat diffusion from the HHSZ might be assisted by intrinsically a very high thermal conductivity of the gneisses in the HHSZ (Ray et al. 2007) as well as heat flow augmented by a number of hot springs (Derry and Evans 2002; Derry et al. 2009). The geothermal gradient data from the HHSZ (Fig. 9) should not be compared with the Prandtl number since they are independent to each other.

Any temporal variation in extrusion of the HHSZ along the orogenic trend was not considered in the flow model in this work (Eq. 1 in 'Appendix 2'). In their flow models, the Dalhousie research group also maintained a constant 1 mm year^{-1} of extrusion rate of the HHSZ (review by Zhang et al. 2004). Along strike variation in structure, topography, precipitation rate, convergence rate, etc. in the Himalaya (e.g. Arora et al. 2012) has no direct bearing on the presented model. Several heterogeneities in deformation at the same location, for example any vertical variation in mechanical property of the rocks (Flesch and Bendick 2012) of the HHSZ as well as its slip rate (see Ponraj et al. 2011) were not taken account. Modern thermal mechanical model of shear zones (e.g. Beaumont et al. 2004; also Kellett et al. 2010—as the latest example) consider a number of other parameters, viz. (i) geothermal gradient, (ii) radioactive heat production at depth, (iii) thermal expansion coefficients of rocks, (iv) change in density during extrusion of rocks and (v) the influence of focused erosion in extrusion. However, following Grasemann et al. (2006), this work neglects these constraints since those do not affect the ductile shear sense (as practiced by Ramsay 1980; Ramsay and Lisle 2000 etc.). Also neglected are (vi) rates of gravity spreading (cf. Ramberg 1981) and erosion of the extruded materials; (vii) kinematic dilatancy (see Fagereng 2012), strain partitioning, strain hardening/softening during shearing (Hobbs et al. 2010); (viii) any variation in slip rate and the resultant pressure gradient over time; (ix) changes in dip amounts of the boundaries of the HHSZ (Jamieson et al. 2004); (x) the upper brittle regime of the HHSZ; (xi) tectonics of any individual unit inside the HHSZ such as the 'Everest Series' and its equivalent units; (xii) pure shear component on the HHSZ; (xiii) structural and thermometric complicacies of the $STDS_U$ (e.g. Carosi et al. 1998; Kellett and Grujic 2012); (xiv) strain localization induced by shear heating (Vauchez et al. 2012) and a possible melt-related weakening (Gerya and Melilick 2011); (xv) any correlation between width of the shear zone and depth (Platt and Behr 2011); and (xvi) the complex interaction between any deformation partitioning and metamorphism (Bell et al. 2012). A similar simplified analytical modelling of ductile shearing was adopted by a number of previous authors (e.g. Koyi 1997; Talbot and Aftabi 2004; Grujic et al. 2002; Mancktelow 2008; Mukherjee and Mulchrone 2012 as few examples).

As depth increases, due to a normal geothermal gradient, density and viscosity are expected to fall. However, assigning a constant viscosity and density of the HHSZ during its extrusion for each set of calculations can be justified at sections where a very low geothermal gradient has been documented such as $\sim$5.5 °C km^{-1} at Sikkim (India, Neogi et al. 1998). But at other sections, where a normal gradient and an abnormally high gradient have been noted (summarized in Fig. 9), the present approach is a simplification.

This work does not produce any new data on the geometry nor slip/extrusion/erosion rates of the HHSZ. Rather, the pre-existing magnitudes of some of these parameters were inserted into the flow equation to estimate a range of viscosity and the Prandtl number of the shear zone. In this calculation, the density and the thermal diffusivity magnitudes were collected from the literatures since their actual ranges of magnitudes in the HHSZ are not known. Using those data along with deduced viscosities, the Prandtl number was obtained. Estimation of a particular geologic parameter with others—one of which is deduced and the other obtained from literatures—is customary in geosciences, such as estimating the exhumation rate from the calculated cooling rate, and a geothermal gradient collected from literature (Bartolini et al. 2003). The presented model accounts for the ductile deformation only and not the shallow-crustal brittle deformation.

Conclusions

The Dalhousie research group proposed and nurtured significantly the concept of channel flow of the Higher Himalayan Shear Zone (HHSZ). Accepting this model as useful, this work estimates the viscosity of the HHSZ along the orogenic trend to be $\sim 10^{16}$–10^{23} Pa s and a Prandtl number of $\sim 10^{21}$–10^{28}. The estimated parameters specifically for the Sutlej section of the HHSZ are $\sim 10^{17}$–10^{23} Pa s and $\sim 10^{22}$–10^{28}. Thus, requirement of a very low viscosity of $\sim 10^{19}$ Pa s for channel flow of south Tibet, as followed by many (e.g. Beaumont et al. 2001; Rey et al. 2010 etc.), from a mid-crustal depth does not hold true. Unlike non-Newtonian rheology assumed in their tectonic models by Whitney et al. (2009), these estimations assume the HHSZ to be a single incompressible Newtonian viscous lithology (similar to many tectonic models as reviewed by Graveleau et al. 2012), bound by parallel boundaries, and use known ranges of slip rates of the boundaries—the Main Central Thrust (Zone) in the south and the ductile shear subzone—South Tibetan Detachment System-Upper ($STDS_U$) in the north, pressure gradients, thicknesses of the HHSZ and that of its subzone $STDS_U$, and the density and the thermal diffusivity of the HHSZ. The last two parameters of the shear zones are taken to range between the maximum and the minimum values of its constituent rocks. The range of viscosity of the HHSZ is broadly in accordance with Copley et al.'s (2011), Rutter et al.'s (2011) and He et al.'s (2012) recent finding of a strong Tibetan mid-crust. The estimated viscosity and the Prandtl number of the HHSZ conform to those for its constituent rocks, the Earth, the continental crust, partly

with the superstructure and party the infrastructure, but not with a granite melt. The high Prandtl number deduced for the HHSZ may be justified by a very limited data on high thermal conductivity of the gneiss of the shear zone.

Wide ranges of thermal and thermo-mechanical parameters of the HHSZ arise due to vast limits on most of its fundamental flow parameters. The present work neglects temporal variation in flow parameters in individual sections. Since this work considers a segment of the HHSZ along the NW–SE trending segment of the Himalayan chain passing through India, Nepal and Bhutan, it does not use extrusion-related parameters from the two syntaxes. Unlike those applied by the Dalhousie school, the present model ignores thermo-mechanical complicacies of the HHSZ. Temporal widening of shear zones (Goncalves et al. 2012) and relationship between deformation and metamorphism (Williams and Jarcinovic 2012) were not investigated for the HHSZ.

Acknowledgments Supported by Department of Science and Technology's (DST, New Delhi) *Fast Track Project* Grant: *SR/FTP/ES-117/2009*. Arundhuti Ghatak (Indian Institute of Scientific Education and Research Bhopal) simplified the language at a few places. Rasmus Thiede (Potsdam University) and Andrew Carter (University of London) made several very crucial constructive comments as informal reviewers. Rajkumar Ghosh (student, IIT Bombay) raised many critical issues. Sidhartha Bhattacharyya (Alabama University) updated with reprints. Barun Kumar Mukherjee (Wadia Institute of Himalayan Geology) is thanked for Guest Editorial handling, Christian Dullo (IFM-Geomar) for Chief Editorial handling, Monika Dullo for her Managing Editorial works and Chris Talbot (retired from Uppsala University) and Rodolfo Carosi (University of Pisa) for comprehensive and exhaustive reviews. Payel Mukherjee did household activities and gave me free time needed to write this paper. IIT Bombay's funding enabled SM to present this work orally (Mukherjee and Mukherjee 2012) in the Himalayan Session: TS 4.5, European Geosciences Union, Vienna. This work is encapsulated in Mukherjee (2012f). Absence of any relevant references in this work is unintentional.

Appendix 1

Questions raised about the channel flow extrusion mechanism of the HHSZ

(i) The 'hairpin' P–T-t path of the Higher Himalaya could also be generated by burial followed by extrusion by any other mechanism (review by Harris 2007). More specifically, the thermal, metamorphic and the chronologic evolution of the Langtang section of the HHSZ in central Nepal fit with the critical taper model. In contrast, the P–T evolution of the Barun Gneiss inside the HHSZ, and the temperature profile from the Karnali section (Nepal) of the HHSZ fit with a channel flow model (Groppo et al. 2012; Yakymchuk and Godin 2012). (ii) The vertical extents of the major Himalayan thrusts at depth are speculative for two reasons. First, the depths that the two faults bounding the HHSZ, viz. the Main Central Thrust (MCT) and the South Tibetan Detachment System-Upper ($STDS_U$), reached and confined the channel flow has remained unconstrained (Sharma 2009). Secondly, whereas in the western Himalaya, the Main Himalayan Thrust (the base of the subhorizontal channel) is well established, its presence in the eastern Himalaya has been questioned by Kayal (2008) based on studies on micro-earthquakes. Finally, at the Kathmandu klippen, the MCT and the leucogranites indicative of channel flow are not observed (Jhonson and Harley 2012); (iii) The geographic extents of partially molten rocks within the Asian as well as the Eurasian plates have remained indeterminate. This is because (iiia) Sudha et al. (2011) deciphered low density materials within fractures near the MCT in the Alaknanda river section (India), and Seshunarayana et al. (2011) from the Bhagirathi section (India); (iiib) based on geochemical studies, Guo and Wilson (2011) recently proposed that the Higher Himalayan leucogranites are derived from a melt of >80 % from the HHSZ itself and <20 % from the Lesser Himalayan rocks by metasomatic replacements. (iiic) a lower crustal zone of low viscosity (of the order of 10^{16} to 10^{17} Pa s) has been envisaged in Mongolia (Vergnolle et al. 2003) but that is ~2,000 km northeast to the HHSZ. (iv) Seismic studies of southern Tibet revealed that the low velocity zones in mid-crust, a possible indicator of rocks in a partially molten state (Zhao et al. 2004), occur as discontinuous pods and cannot support channel flow throughout the Himalaya (Hetényi et al. 2011; Zhang et al. 2012). A 'soft Tibet' model required for channel flow is not supported by geophysical evidences (Tapponnier 2012). (v) A low Poisson's ratio of 0.24 below NE Tibet possibly indicates a felsic rheology devoid of any flow (Pan and Niu 2011). (vi) Crustal thickness of the Tibet can be explained by Cenozoic shortening and channel flow is not a requisite (Lease et al. 2012 and references therein). Harrison (2006) argued that (viia) the crustal low velocity zone could be due to aqueous phases rather than partially molten rocks (also, reviews by Unsworth 2010, Yang et al. 2012); and (viib) no zircon from the Gangdese batholith, characteristic of the partially molten rocks, has been documented from the HHSZ. However, Jamieson et al. (2006) negated the second argument by using the 'material tracking method' of modelling to show that ~30 Ma of channel flow could not expose the Asian materials on the surface. Though it is still unclear whether the low velocity zone below the southern Tibet is a genuine indication of partially molten rocks (Bai et al. 2010's review), a mixture of aqueous phases and partially molten rocks can also sustain a flow (Unsworth 2010).

(viii) Finite element modelling of the Tibetan tectonics reveals a high viscosity of $\sim 5 \times 10^{23}$ Pa s at mid-crustal depth, much higher than a previous estimate of 10^{19}–10^{21} Pa s by Hilley et al. (2005), which has been considered to be unsuitable for channel flow (Copley et al. 2011).

(ix) Considering the rate of uplift and the elevation of the Tibetan plateau, Rey et al. (2010) deduced a Moho temperature of 500–600 °C before the plateau thickened. This temperature was considered by them unsuitable for a long-distance channel flow. (x) Based on U-Th–Pb monazite dates, it has been shown that the HHSZ in the eastern Himalaya extruded by channel flow and critical taper mechanisms in a flipping mode (Beaumont and Jamieson 2010; Chambers et al. 2011). This could hold true for the Himalayan orogen where protracted erosion between ~16–18 Ma and at ~3 Ma led to channel flow, and waning of erosion in the intervening phases allowed a critical taper situation (Beaumont and Jamieson 2010; Clift 2010). Even if one considers that channel flow operated within certain time intervals, whether it is persisting at present is unknown (Kohn 2008; Imayama et al. 2010). (xi) Lithological correlation between the Indian basement and the Himalaya led Yin et al. (2007) to conclude that unlike channel flow, the eastern Himalaya underwent thick skinned tectonics. (xii) Integrating structural, metamorphic and tectonic data, Herman et al. (2010) favoured the 'duplex model' over the channel flow model. (xiii) Carosi et al. (2010) argued that merely 2- to 4-km-thick Higher Himalayan Crystalline in Lower Dolpo (western Nepal) cannot support channel flow. Secondly, activation of the Toijem Shear Zone inside the Higher Himalaya at ~26 Ma much before than that of the MCTZ and the $STDS_U$ at ~23–17 Ma does not fit with a simple channel flow of the Higher Himalaya there. (xiv) The channel flow model assumes that flow takes place inside rigid boundaries. However, Mandal et al. (2009) argued that phyllites of the Daling Group as the lower boundary of the channel in the Sikkim–Darjeeling Himalaya is deformed ductilely and did not act as a rigid block; (xv) A zone of flexure slip fold inside the HHSZ in the Dhauliganga section (India) indicated that mere channel flow probably did not operate in that section (Mukherjee 2010c). (xvi) Whether the channel flow can model explain the genesis of sigmoidal, parallelogram and lenticular shear fabrics inside the HHSZ has been questioned (Mukherjee 2009; Mukherjee and Koyi 2010a, b) but not investigated. (xvii) In their fig. 11c, White et al. (2012) demonstrated that slab rollback can well explain Himalayan gneiss domes without any need to introduce channel flow.

Appendix 2

The 'Poisson equation' of rectilinear flow of an incompressible Newtonian viscous fluid in the z-direction through a very long parallel rigid boundary inclined shear zone is given by (Eq. 6.190 of Papanastasiou et al. 2000):

$$(\partial^2 U_z/\partial x^2) + (\partial^2 U_z/\partial y^2) = \mu^{-1}[\partial P/\partial z - dg\ \mathrm{Sin}\theta] \quad (1)$$

'x' and 'y' are perpendicular directions that lie on the cross-section of the shear zone; U_z—fluid along z-direction; 'μ'—fluid viscosity; $(\partial P/\partial x)$—pressure gradient leading t o extrusion; 'd': fluid density; 'g': gravitational acceleration; and 'θ': shear zone dip.

Considering only the YZ section, $(\partial^2 U_z/\partial x^2) = 0$. Therefore:

$$(\partial^2 U_z/\partial y^2) = \mu^{-1}[\partial P/\partial z - d\,g\ \mathrm{Sin}\theta] \quad (2)$$

Integrating twice, considering the shear zone to be of $2y_0$ units thick, and at $y = y_0$, $U_z = -U_1$ and at $y = -y_0$, $U_z = U_2$ gives the profile:

$$U_z = 0.5\mu^{-1}(\partial P/\partial z - d\,g\ \mathrm{Sin}\theta)\left(y^2 - y_0^2\right) + 0.5\left\{(U_2 - U_1) - y\,y_0^{-1}(U_1 + U_2)\right\} \quad (3)$$

Being a quadratic equation, it represents a parabola, whose vertex has the following coordinate:

x-ordinate: $0.5\ (U_1 - \mathrm{U}_2) + 0.125\ \mu\ y_0^{-2}\ (U_1 + U_2)^2\ (\partial P/\partial z - d\ g\ \mathrm{Sin}\theta)^{-1} - 0.5\ y_0^2\ \mu^{-1}\ (\partial P/\partial z - d\ g\ \mathrm{Sin}\theta)$

y-ordinate: $0.5\ \mu\ y_0^{-1}\ (U_1 + U_2)\ (\partial P/\partial z - d\ g\ \mathrm{Sin}\theta)^{-1}$

The vertex lies inside the shear zone if

$$y_0 > 0.5\mu y_0^{-1}(U_1 + U_2)(\partial P/\partial z - d\,g\ \mathrm{Sin}\theta)^{-1} \quad (4)$$

It lies on one of the boundaries if

$$y_0 = 0.5\mu y_0^{-1}(U_1 + U_2)(\partial P/\partial z - d\,g\ \mathrm{Sin}\theta)^{-1} \quad (5)$$

And it lies outside the shear zone if

$$y_0 < 0.5\mu y_0^{-1}(U_1 + U_2)(\partial P/\partial z - d\,g\ \mathrm{Sin}\theta)^{-1} \quad (6)$$

In case of Eq. (4), the thickness of the $STDS_U$ is

$$T = [y_0 - -0.5\mu y_0^{-1}(U_1 + U_2)(\partial P/\partial z - d\,g\ \mathrm{Sin}\theta)^{-1}]. \quad (7)$$

References

Amidon WH, Burbank DW, Gehrels GE (2005) U-Pb zircon ages as a sediment mixing tracer in the Nepal Himalaya. Earth Planet Sci Lett 235:244–260

Annen C, Scaillet B (2006) Thermal evolution of leucogranites in extensional fault: implications for Miocene denudation rates in the Himalaya. In: Law RD, Searle MP, Godin L (eds) Channel flow, ductile extrusion and exhumation in continental collision zones. J Geol Soc London, Sp Pub, 268:309–326

Annen C, Scaillet B, Sparks RSJ (2006) Thermal constraints on the emplacement rate of a large intrusive complex: the Manaslu Leucogranite, Nepal Himalaya. J Petrol 47:71–95

Argles T (2011) Geology on the world's roof. Geoscientist 21:12–16

Arora BR, Gahalaut VK, Kumar N (2012) Structural control on along-strike variation in the seismicity of the Northwest Himalaya. J Asian Earth Sci (in press)

Bai D, Unsworth MJ, Meju MA et al (2010) Crustal deformation of the eastern Tibetan plateau revealed by magnetotelluric imaging. Nat Geosci 3:358–362

Barraud J, Gardien V, Allemand P et al (2004) Analogue models of melt-flow networks in folding migmatites. J Struct Geol 26:307–324

Bartolini C, D'Agostino N, Dramis F (2003) Topography, exhumation and drainage network evolution of the Apennines. Episodes 26:212–216

Beaumont C, Ings SJ (2012) Effect of depleted continental lithosphere counterflow and inherited crustal weakness on rifting of the continental lithosphere: general results. J Geophys Res (in press)

Beaumont C, Jamieson RA (2010) Himalayan-Tibetan Orogeny: channel flow versus (critical) wedge models, a false dichotomy? In: Leech ML et al (eds) Proceedings for the 25th Himalaya-Karakoram-Tibet Workshop: U.S. Geological Survey, Open-File Report 2010–1099, 2 p. URL: http://pubs.usgs.gov/of/2010/1099/beaumont/

Beaumont C, Jamieson RA, Nguyen MH et al (2001) Himalayan tectonics explained by extrusion of a low-viscosity crustal channel coupled to focused surface denudation. Nature 414:738–742

Beaumont C, Jamieson RA, Nguyen MH et al (2004) Crustal channel flows: 1. Numerical models with applications to the tectonics of the Himalayan-Tibet orogen. J Geophys Res 109:B06406

Beaumont C, Nguyen M, Jamieson RA et al (2006) Crustal flow modes in large hot orogens. In: Law RD, Searle MP, Godin L (eds) Channel flow, Ductile Extrusion and Exhumation in Continental Collision Zones. Geol Soc London. Spec vol 268, pp 91–145

Beaumont C, Jamieson RA, Nguyen MH et al (2007) Erosion-induced reactivation of the Main Central Thrust zone: Model and implications for channel flow in the Himalaya-Tibet system. Am Geophys Union. Fall Meeting. Abstract # T34C-01 URL: http://adsabs.harvard.edu/abs/2007AGUFM.T34C.01B

Beaumont C, Jamieson RA, Butler JP et al (2009) Crustal structure: a key constraint on the mechanism of ultra-high-pressure rock exhumation. Earth Planet Sci Lett 287:116–129

Bell TH, Sapkota J (2012) Episodic gravitational collapse and migration of the mountain chain during orogenic roll-on in the Himalayas. J Meta Geol 30:651–666

Bell TH, Rieuwers M, Cihan M et al (2012) Inter-relationships between deformation partitioning, metamorphism and tectonism. Tectonophysics (in press)

Bhattacharya AR (1999) Deformational regimes across the Kumaun Himalaya: a study in strain patterns. In: Jain AK, Manickavasagam RM (eds) Geodynamics of the NW Himalaya. Gond Res Gp Mem No 6 Field Science, Osaka, pp 81–90

Bott MHP (1971) The interior of the earth. Edward Arnold Publishers, London

Boyd FR, Meyer HOA (1979) The mantle sample: inclusions in kimberlites and other volcanics. American Geophysical Union (AGU), Washington, DC. doi:10.1029/SP016

Brewer ID, Burbank DW, Hodges KV (2006) Downstream development of a detrital cooling-age signal: Insights from $^{40}Ar/^{39}Ar$ muscovite thermochronology in the Nepalese Himalaya. In: Willett SD, Hovius N, Brandon MT et al (eds) Tectonics, Climate, and Landscape Evolution. Geol Soc Am Spec Pap 398:321–338

Buntebarth G (1984) Geothermics. Springer, New York

Burbank DW (2005) Earth science: cracking the Himalaya. Nature 434:963–964

Burbank DW, Anderson RS (2012) Tectonic geomorphology, 2nd edn. Wiley-Blackwell, Oxford, pp 14–16

Burchfiel BC, Chen Z, Hodges KV et al (1992) The South Tibet Detachment System, Himalayan orogen: extension contemporaneous with and parallel to shortening in a collisional mountain belt. Geol Soc Am Spec Pap 269:1–41

Caldwell WB, Klemperer SL, Rai SS et al (2009) Partial melt in the upper-middle crust of the northwest Himalaya revealed by Rayleigh wave dispersion. Tectonophysics 477:58–65

Carmichael RS (1989) Practical handbook of physical properties of rocks & minerals. CRC Press, Boca Raton

Carosi RB, Lombardo G, Molli G et al (1998) The South Tibetan Detachment System in the Rongbuk valley, Everest region: deformation features and geological implications. J Asian Earth Sci 16:299–311

Carosi R, Musumeci G, Pertusali PC (1999) Extensional tectonics in the higher Himalayan Crystallines of Khumbu Himal, eastern Nepal. In: Macfarlane A, Sorkhabi RB, Quade J (eds) Himalaya and Tibet: mountain roots to mountain tops, 328. Geological Society of London, Sp Pub, Boluder, Colorado, pp 211–223

Carosi R, Montomoli C, Visonà D (2002) Is there any detachment in the Lower Dolpo (western Nepal)? C R Geosci 334:933–940

Carosi R, Montomoli C, Rubatto D et al (2006) Normal-sense shear zones in the core of the Higher Himalayan Crystallines (Bhutan Himalaya): evidence for extrusion? In: Law RD, Searle MP, Godin L (eds) Channel Flow, Ductile Extrusion and Exhumation in Continental Collision Zones. Geol Soc, London, Spec Publ 268:425–444

Carosi R, Montomoli C, Visonà D (2007) A structural transect in the lower Dolpo: insights in the tectonic evolution of Western Nepal. J Asian Earth Sci 29:407–423

Carosi R, Montomoli C, Rubatto D et al (2010) Late Oligocene high-temperature shear zones in the core of the Higher Himalayan Crystallines (Lower Dolpo, western Nepal). Tectonics 29:TC4029

Carter A, Foster GL (2009) Improving constraints on apatite province: Nd measurement on fission-track dated grains. In: Lisker F, Ventura B, Glasmacher UA (eds) Thermochronological methods: from paleotemperature constraints to landscape evolution models. Geol Soc, London Spec Pub 324:57–72

Catlos EJ, Harrison TM, Kohn MJ (2001) Geochronologic and thermobarometric constraints on the evolution of the Main Central Thrust, central Nepal Himalaya. J Geophys Res 106:16177–16204

Chakungal J, Dostal J, Grujic D et al (2010) Provenance of the Greater Himalayan sequence: evidence from mafic granulites and amphibolites in NW Bhutan. Tectonophysics 480:198–212

Chambers JA, Argles TW, Horstwood MSA et al (2008) Tectonic implications of Palaeoproterozoic anatexis and Late Miocene metamorphism in the Lesser Himalayan Sequence, Sutlej valley, NW India. J Geol Soc Lond 165:725–737

Chambers J, Parrish R, Argles T et al (2011) A short duration pulse of ductile normal shear on the outer South Tibetan detachment in Bhutan: alternating channel flow and critical taper mechanics of the eastern Himalaya. Tectonics 30:TC2005

Chatterjee S, Goswami A, Scotese CR (2012) The longest voyage: tectonic, magmatic, and paleoclimatic evolution of the Indian plate during its northward flight from Gondwana to Asia. Gond Res (in press)

Chen J-L, Xu J-F, Zhao W et al (2011) Geochemical variations in Miocene adakitic rocks from the western and eastern Lhasa terrane: implications for lower crustal flow beneath the Southern Tibetan Plateau. Lithos 125:9928–9939

Clift PD (2010) Enhanced global continental erosion and exhumation driven by Oligo-Miocene climate change. Geophys Res Lett 37:L09402

Clift PD, Plumb A (2008) The Asian monsoon: causes history and effects. Cambridge University Press, Cambridge

Clift PD, Giaosan L, Carter A et al (2010) Monsoon control over erosion patterns in the western Himalaya: possible feed-back into the tectonic evolution. In: Clift PD, Tada R, Zheng H (eds)

Monsoon evolution and tectonics-climate linkage in Asia. Geol Soc, London, Spec Publ 342:185–218
Copley A, Avouac J-P, Wernicke BP (2011) Evidence for mechanical coupling and strong Indian lower crust beneath southern Tibet. Nature 472:79–81
Corrie SL, Kohn MJ (2011) Metamorphic history of the Central Himalaya, Annapurna region, Nepal, and implications for tectonic models. Geol Soc Am Bull 123:1863–1879
Cottle JM, Jessup MJ, Newell DL et al (2007) Structural insights into the early stages of exhumation along an orogen-scale detachment: the South Tibetan Detachment System, Dzakaa Chu section, Eastern Himalaya. J Struct Geol 29:1781–1797
Daniel CG, Hollister LS, Parrish RR et al (2003) Exhumation of the Main Central Thrust from Lower Crustal depths, Eastern Bhutan Himalaya. J Meta Geol 21:317–334
Davidson C, Smith SM, Hollister LS (1994) Role of melt during deformation in the deep crust. Terra Nova 6:133–142
Davies PA (1980) Laboratory modelling of mantle flows. In: Davies PA, Runcorn SK (eds) Mechanisms of continental drift and plate tectonics. Academic Press, London, pp 225–244
Davies GF (2001) Dynamic earth, plates, plumes and mantle convection. Cambridge University Press, Cambridge
de Sigoyer J, Guillot G, Dick P (2004) Exhumation of the ultrahigh-pressure Tso Morari unit in eastern Ladakh (NW Himalaya): a case study. Tectonics 23:TC3003
Dennis JG (1987) Structural geology an introduction. Wm C Brown Publishers, Dubuque
Derry LA, Evans MJ (2002) Geochemical constraints on geothermal heat flow in the central Nepal Himalaya. American Geophysical Union, Fall Meeting, Abstract #T71A-1163
Derry LA, Evans MJ, Darling R et al (2009) Hydrothermal heat flow near the Main Central Thrust, central Nepal Himalaya. Earth Planet Sci Lett 286:101–109
Dewei L (2008) Continental lower-crustal flow: channel flow and laminar flow. Earth Sci Frontiers 15:130–139
Dézes PJ, Vannay JC, Steck A et al (1999) Synorogenic extension: quantitative constraints on the age and displacement of the Zanskar shear Zone. Geol Soc Am Bull 111:364–374
Dong S (2002) On continent-continent point-collision and ultrahigh-pressure metamorphism. Acta Geol Sinica 76:69–80
Edwards RM (1995) $^{40}Ar/^{39}Ar$ geochronology of the Main Central Thrust (MCT) region; evidence for late Miocene to Pliocene disturbances along the MCT, Marsyandi River valley, westcentral Nepal Himalaya. J Nepal Geol Soc 10:41–46
Ernst WG, Liou JG (2008) High- and ultrahigh-pressure metamorphism—past results and future prospects. Am Miner 93:1771–1786
Faccenda M, Gerya TV, Chakraborty S (2008) Styles of post subduction collisional orogeny: influence of convergence velocity, crustal rheology and radiogenic heat production. Lithos 103:257–287
Fagereng Å (2012) On stress and strain in a continuous-discontinuous shear zone undergoing simple shear and volume loss. J Struct Geol (in press)
Flesch L, Bendick R (2012) The relationship between surface kinematics and deformation of the whole lithosphere. Geology 40:711–714
Fowler CMR (2005) The solid earth, an introduction to global geophysics. Cambridge University Press, Cambridge, pp 294–358
Francsis MK (2012) Piezometry and Strain Rate Estimates Along Mid-Crustal Shear Zones. Thesis: Master of Science in Geosciences. Virginia Polytechnic Institute and State University, pp 1–110
Fraser G, Worley B, Sandiford M (2000) High-precision geothermometry across the High Himalayan metamorphic sequence, Langtang Valley, Nepal. J Meta Geol 18:665–681
Ganguly J, Dasgupta S, Cheng W et al (2000) Exhumation history of a section of the Sikkim Himalayas, India: records in the metamorphic mineral equilibria and compositional zoning of garnet. Earth Planet Sci Lett 183:471–486
Gansser A (1964) The geology of the Himalayas. Wiley Interscience, New York
Gehrels G, Kapp P, DeCelles P et al (2011) Detrital zircon geochronology of pre-Tertiary strata in the Tibetan–Himalayan orogens. Tectonics 30:TC5016
Gerya TV, Meilick FI (2011) Geodynamic regimes of subduction under an active margin: effects of rheological weakening by fluids and melts. J Meta Geol 29:7–31
Gerya TV, Perchuk LL, van Reenan DD, Smit CA (2000) Two-dimensional numerical modeling of pressure ± temperature-time paths for the exhumation of some granulite facies terrains in the Precambrian. J Geodyn 30:17–35
Giambiagi L, Mescua J, Bechis F et al (2012) Thrust belts of the southern Central Andes: Along-strike variations in shortening, topography, crustal geometry and denudation. GSA Bull 124: 1339–1351
Godard V, Burbank DW (2011) Mechanical analysis of controls on strain partitioning in the Himalayas of Central Nepal. J Geophys Res 116:B10402
Godin L, Grujic D, Law RD et al (2006) Channel flow, extrusion and extrusion in continental collision zones: an introduction. In: Law RD, Searle MP (eds) Channel flow, extrusion and extrusion in continental collision zones. Geol Soc Lond Spec Publ 268:1–23
Goncalves P, Oliot E, Marquer D et al (2012) Role of chemical processes on shear zone formation: an example from the Grimsel metagranodiorite (Aar massif, Central Alps). J Meta Geol 30: 703–722
Gong J, Ji J, Han B et al (2012) Early subduction–exhumation and late channel flow of the Greater Himalayan Sequence: implications from the Yadong section in the eastern Himalaya. Int Geol Rev 54:1184–1202
Goscombe B, Hand M (2000) Contrasting P-T Paths in the Eastern Himalaya, Nepal: inverted isograds in a paired metamorphic mountain belt. J Petrol 41:1673–1719
Goscombe B, Gray D, Hand M (2006) Crustal architecture of the Himalayan metamorphic front in eastern Himalaya. Gond Res 10:232–255
Grasemann B (1993) Numerical modeling of the thermal history of the NW Himalaya, Kullu valley, India. In: Treloar PJ, Searle MP (eds) Himalayan Tectonics. Geol Soc Sp Pub No 74:475–484
Grasemann B, Fritz H, Vannay JC (1999) Quantitative kinematic flow analysis from the Main Central Thrust Zone (NW-Himalaya, India): implications for a decelerating strain path and extrusion of orogenic wedges. J Struct Geol 21:837–853
Grasemann B, Edwards MA, Wiesmayr G (2006) Kinematic dilatancy effects on orogenic extrusion. In: Law RD, Searle MP, Godin L (eds) Channel flow, ductile extrusion and exhumation in continental collisional zones, vol 268. Geological Society of London, Special Publication, pp 183–199
Graveleau F, Malavieille J, Dominguez S (2012) Experimental modelling of orogenic wedges: a review. Tectonophysics 538–540:1–66
Gray R, Pysklywec RN (2012) Geodynamic models of mature continental collision: evolution of an orogen from lithospheric subduction to continental retreat/delamination. J Geophys Res 117:B03408
Groppo C, Rolfo F, Indares A (2012) Partial Melting in the Higher Himalayan Crystallines of Eastern Nepal: the effect of decompression and implications for the 'Channel Flow' Model. J Petrol (in press)
Grujic D (2006) Channel flow and continental collision tectonics: an overview. In: Law RD, Searle MP (eds) Channel flow, extrusion

and exhumation in continental collision zones. Geol Soc Lond Spec Publ 268:25–37
Grujic D, Casey M, Davidson C et al (1996) Ductile extrusion of the Higher Himalayan crystalline in Bhutan: evidence from quartz microfabrics. Tectonophysics 260:21–43
Grujic D, Hollister LS, Parrish RR (2002) Himalayan metamorphic sequence as an orogenic channel: insight from Bhutan. Earth Planet Sci Lett 198:177–191
Grujic D, Beaumont C, Jamieson RA et al (2004) Types of processes in crustal channels evidenced by along-strike variations in the tectonic style of the Himalayas and by numerical models. In: Channel flow, ductile extrusion and exhumation of lower-mid crust in continental collision zones, Royal Society, London. Abstract volume
Grujic D, Coutand I, Bookhagen B et al (2006) Climatic forcing of erosion, landscape, and tectonics in the Bhutan Himalayas. Geology 34:801–804
Grujic D, Warren CJ, Wooden JL (2011) Rapid synconvergent exhumation of Miocene-aged lower orogenic crust in the eastern Himalaya. Lithosphere 3:344–346
Guilmette C, Indares A, Hébert R (2011) High-pressure anatectic paragneisses from the Namche Barwa, Eastern Himalayan Syntaxis: textural evidence for partial melting, phase equilibria modeling and tectonic implications. Lithos 124:66–81
Gunzburger Y (2010) Stress state interpretation in light of pressure-solution creep: numerical modelling of limestone in the Eastern Paris Basin, France. Tectonophysics 483:377–389
Guo Z, Wilson M (2011) The Himalayan leucogranites: constraints on the nature of their crustal source region and geodynamic setting. Gond Res 22:360–376
Guo Z, Gao X, Wang W et al (2012) Upper- and mid-crustal radial anisotropy beneath the central Himalaya and southern Tibet from seismic ambient noise tomography. Geophys J Int 189:1169–1182
Gupta S, Das A, Goswami S et al (2010) Evidence for structural discordance in the inverted metamorphic sequence of the Sikkim Himalaya: towards resolving the MCT controversy. J Geol Soc India 75:313–322
Harris N (2007) Channel flow and the Himalayan-Tibetan orogen: a critical review. J Geol Soc London 164:511–523
Harris N (2008) Processes during continental collision. Chapter 6. In: Rogers N, Blake S (eds) An introduction to our dynamic planet, pp 241–272
Harrison TM (2006) Did the Himalayan Crystallines extrude partially molten from beneath the Tibetan Plateau? In: Law, RD, Searle MP, Godin L (eds) Channel flow, ductile extrusion and exhumation in continental collision zones, vol 268. Geological Society, London, Special Publications, pp 237–254
Harrison TM, Ryerson FJ, Le Fort P et al (1997) A Late Miconce-Pliocene origin for the Central Himalayan inverted metamorphism. Earth Planet Sci Lett 146:E1–E7
Hatzfeld D, Molnar P (2010) Comparisons of the kinematics and deep structures of the Zagros and Himalaya and of the Iranian and Tibetan plateaus and geodynamic implications. Rev Geophys 48:RG2005
Hauck ML, Nelson KD, Brown LD et al (1998) Crustal structure of the Himalayan orogen at 900 east longitude from project INDEPTH deep seismic reflection profiles. Tectonics 17:481–500
He J, Lu S, Wang W (2012) Three-dimensional mechanical modeling of the GPS velocity field around the northeastern Tibetan plateau and surrounding regions. Tectonophysics (in press)
Heim A, Gansser A (1939) Central Himalaya: geological observations of the Swiss expedition, pp 1–246
Henderson P, Henderson GM (2009) The Cambridge handbook of earth science data. Cambridge University Press, Cambridge
Herman F, Copeland P, Avouac J-P et al (2010) Exhumation, crustal deformation, and thermal structure of the Nepal Himalaya derived from the inversion of thermochronological and thermobarometric data and modeling of the topography. J Geophys Res 115:B06407
Herren E (1987) Zanskar Shear Zone: northeast southwest extension within the Higher Himalaya (Ladakh, India). Geology 15:409–413
Hetényi G., Vergne J, Bollinger L et al (2011) Discontinuous low-velocity zones in southern Tibet question the viability of the channel flow model. Discontinuous low-velocity zones in southern Tibet question the viability of the channel flow model. In: Gloaguen R, Ratschbacher L (eds) Growth and Collapse of the Tibetan Plateau. Geol Soc London, Spec Publ 353:99–108
Heuze FE (1983) High-temperature mechanical, physical and thermal properties of granitic rocks. A review. Int J Rock Mech Min Sci Geomech Abstr 20:3–10
Hilley GE, Burgmann R, Zhang PZ, Molnar P (2005) Bayesian inference of plastosphere viscosities near the Kunlun Fault, northern Tibet. Geophys Res Lett 32:L01302
Hindle D (2003) Finite strain variations along strike in mountain belts. In: Nieuwland DA (ed) New insights into structural interpretation and modelling. Geol Soc London Sp Pub 212:59–74
Hobbs, BE, Ord A, Spalla MI et al (2010) The interaction of deformation and metamorphic reactions. In: Spalla MI, Marotta AM, Gosso G (eds) Advances in interpretation of geological processes: refinement of multiscale data and integration in numerical modelling. Geol Soc London Spec Publ 332:189–223
Hodges KV (2006) A synthesis of the channel flow-extrusion hypothesis as developed for the Himalayan-Tibetan orogenic system. In: Law RD, Searle MP (eds) Channel flow, extrusion and exhumation in continental collision zones. Geol Soc Lond Spec Publ 268:71–90
Hodges K, Bowring S, Davidek K et al (1998) Evidence for rapid displacement on Himalayan normal faults and the importance of tectonic denudation in the evolution of mountain ranges. Geology 26:483–486
Hollister LS, Grujic D (2006) Himalaya Tiber Plateau. Pulsed channel flow in Bhutan. In: Law RD, Searle MP, Godin L (eds) Channel flow, ductile extrusion and exhumation in continental collision zones, vol 268. Geol Soc London, Sp Pub, pp 415–423
Hubbard MS (1996) Ductile shear as a cause of inverted metamorphism: example from the Nepal Himalaya. J Geol 104:493–499
Hubbard MS, Harrison TM (1989) 40Ar/39Ar age constraints on deformation and metamorphism in the MCT Zone and Tibetan Slab, eastern Nepal Himalaya. Tectonics 8:865–880
Huetra AD, Royden LH, Hodges KV (1999) The effects of accretion, erosion and radiogenic heat on the metamorphic evolution of collision orogens. J Meta Geol 17:349–366
Huntington KW, Blythe AE, Hodges KV (2006) Climate change and Late Pliocene acceleration of erosion in the Himalaya. Earth Planet Sci Lett 252:107–118
Imayama T, Takeshita T, Arita K (2010) Metamorphic P-T profile and P–T path discontinuity across the far-eastern Nepal Himalaya: investigation of channel flow models. J Meta Geol 28:527–549
Imayama T, Takeshita T, Yi K (2011) Two-stage partial melting and contrasting cooling history within the Higher Himalayan Crystalline Sequence in the far-eastern Nepal Himalaya. Lithos 134–135:1–22
Jain AK, Anand A (1988) Deformational and strain patterns of an intracontinental ductile shear zone- an example from the Higher Garhwal Himalaya. J Struct Geol 10:717–734
Jain AK, Patel RC (1999) Structure of the Higher Himalayan Crystallines along the Suru-Doda Valleys (Zanskar),

NWHimalaya. In: Jain AK, Manickavasagam RM (eds) Geodynamics of the NW Himalaya. Gond Res Gp Mem No 6. Field Science, Osaka, pp 91–110
Jain AK, Singh S, Manickavasagam RM (2002) Himalayan collisional tectonics. Gond Res Gp Mem No. 7. Field Science, Hashimoto
Jamieson RA, Beaumont C, Medvedev S et al (2004) Crustal channel flows: 2. Numerical models with implications for metamorphism in the Himalayan–Tibetan Orogen. J Geophys Res 109:B06407
Jamieson RA, Beaumont C, Nguyen MH et al (2006) Provenance of the Greater Himalayan Sequence and associated rocks: Predictions of channel flow models. In: Law RD, Searle MP (eds) Channel flow, extrusion and extrusion in continental collision zones. Geol Soc Lond Spec Publ 268:165–182
Jamieson R, Unsworth MJ, Harris NBW et al (2011) Crustal melting and the flow of mountains. Elements 7:253–260
Jarvis GT, Peltier WR (1989) Convection models and geophysical observation. In: Peltier WR (ed) Mantle convection. Gordon and Breach Science Publisher, New York, pp 479–594
Jaupart C, Mareschal J-C (2011) Cambridge University Press, pp 50
Jessup MJ, Cottle JM (2010) Progression from south-directed extrusion to orogen-parallel extension in the southern margin of the Tibetan Plateau, Mount Everest Region, Tibet. J Geol 118:467–486
Jessup MJ, Law, RD, Searle MP et al (2006) Structural evolution and vorticity of flow during extrusion and exhumation of the Greater Himalayan Slab, Mount Everest Massif, Tibet / Nepal; implications for orogen-scale flow partitioning. In: Law RD, Searle MP, Godin L (eds) Channel flow, ductile extrusion and exhumation in continental collision zones, Geological Society, London, Special Publications 268, pp 379–413
Jessup MJ, Cottle JM, Searle MP et al (2008) P–T–t–D paths of Everest Series schist, Nepal. J Meta Geol 26:717–739
Johnson MRW (2002) Shortening budgets and the role of continental subduction during the India–Asia collision. Earth Sci Rev 59:101–123
Johnson MRW, Harley SL (2012) Orogenesis: the making of mountains. Cambridge University Press, Cambridge, pp 179–192
Johnson SE, Lenferink HJ, Marsh JH et al (2009) Kinematic vorticity analysis and evolving strength of mylonitic shear zones: new data and numerical results. Geology 37:1075–1078
Jones RR, Holdsworth RE, Hand M et al (2006) Ductile extrusion in continental collision zones: ambiguities in the definition of channel flow and its identification in ancient orogens. In: Law RD, Searle MP, Godin L (eds) Channel flow, ductile extrusion and exhumation in continental collision zones, Geological Society, London, Special Publications 268, pp 201–219
Kayal J (2008) Great Himalayan earthquakes and conceptual tectonic models. In: Session: ASI-07 The Himalayas and neighbouring regions. 33rd International Geological Congress, Oslo, Norway
Keary P, Klepeis KA, Vine FJ (2009) Global tectonics, 3rd edn. Wiley-Blackwell, Oxford
Kellett DA, Godin L (2009) Pre-Miocene deformation of the Himalayan superstructure, Hidden valley, central Nepal. J Geol Soc 166:261–275
Kellett DA, Grujic D (2012) New insight into the South Tibetan detachment system: not a single progressive deformation. Tectonics 31:TC2007
Kellett DA, Grujic D, Warren C et al (2010) Metamorphic history of a syn-convergent orogen parallel detachment: the South Tibetan detachment system, Bhutan Himalaya. J Meta Geol 28:785–808
Kohn MJ (2008) P-T-t data from central Nepal support critical taper and repudiate large-scale channel flow of the Greater Himalayan Sequence. GSA Bull 120:259–273
Kohn MJ, Corrie SL (2011) Preserved Zr-temperatures and U-Pb ages in high-grade metamorphic titanite: evidence for a static hot channel in the Himalayan orogen. Earth Planet Sci Lett 311:136–143
Kohn MJ, Wieland MS, Parkinson CD et al (2004) Miocene faulting at plate tectonic velocity in the Himalaya of central Nepal. Earth Planet Sci Lett 228:299–310
Koyi HA (1997) Analogue modelling: from a qualitative to a quantitative technique, a historical outline. J Petrol Geol 20:223–238
Kukkonen IT, Jokinen J, Seipold U (1999) Temperature and pressure dependencies of thermal transport properties of rocks: implications for uncertainties in thermal lithosphere models and new laboratory measurements of high-grade rocks in the central Fennoscandian shield. Surv Geophys 20:53–59
Landholt-Bornstein (1982) Numerical data and functional relationships in Science and Technology. In: Angenheister G (ed) Physical properties of rocks, subvolume A. vol 1. Springer, Berlin, pp 103, 116
Lappa M (2010) Thermal convection: patterns, evolution and stability, pp 103
Larson KP, Godin L (2009) Kinematics of the Greater Himalaya sequence, Dhaulagiri Himal: implications for the structural framework of central Nepal. J Geol Soc Lond 166:25–43
Larson KP, Godin L, Price RA (2010) Relationships between displacement and distortion in orogens: linking the Himalayan foreland and hinterland in central Nepal. GSA Bull 122:1116–1134
Law RD, Searle MP, Simpson RL (2004) Strain, deformation temperatures and vorticity of flow at the top of the Greater Himalayan Slab, Everest Massif, Tibet. J Geol Soc Lond 161:305–320
Law R, Stahr III DW, Ahmad T et al (2010) Deformation Temperatures and Flow Vorticities Near the Base of the Greater Himalayan Crystalline Sequence, Sutlej Valley and Shimla Klippe, NW India. In Leech ML et al (eds) Proceedings for the 25th Himalaya-Karakoram-Tibet Workshop: U.S. Geological Survey, Open-File Report 2010–1099, 2 p. URL: http://pubs.usgs.gov/of/2010/1099/law/
Law RD, Jessup MJ, Searle MP et al (2011a) Telescoping of isotherms beneath the South Tibetan Detachment System, Mount Everest Massif. J Struct Geol 33:1569–1594
Law R, Stahr D, Grasemann B et al (2011) Deformation temperatures and flow vorticities near the base of the Greater Himalayan Crystalline Sequence, Sutlej Valley and Shimla Klippe, NW India. Geophys Res Abstracts, European Geoscicnes Union General Assembly Vol 13 URL: http://meetingorganizer.copernicus.org/EGU2011/EGU2011-2300.pdf
Lease RO, Burbank DW, Zhang H et al (2012) Cenozoic shortening budget for the northeastern edge of the Tibetan Plateau: is lower crustal flow necessary? Tectonics 31:TC3011
Leech ML, Singh S, Jain AK et al (2005) The onset of the India–Asia continental collision: early, steep subduction required by the timing of UHP metamorphism in the western Himalaya. Earth Planet Sci Lett 234:83–97
Leloup PH, Mahéo G, Arnaud E et al (2010) The South Tibet detachment shear zone in the Dinggye area Time constraints on extrusion models of the Himalayas. Earth Planet Sci Lett 292:1–16
Liu M, Yang Y (2003) Extensional collapse of the Tibetan plateau: results of three dimensional finite element modelling. J Geophys Res 108:2361
Lombardo B, Pertusati P, Borghi S (1993) Geology and tectonomagmatic evolution of the eastern Himalaya along the Chomolungma-Makalu transect. In: Treloar PJ, Searle MP (eds) Himalayan Tectonics. The Geological Society Special Publication, vol 74, pp 341–355

Long S, Mcquarrie N, Tobgay T et al (2011) Geometry and crustal shortening of the Himalayan fold-thrust belt, eastern and central Bhutan. Geol Soc Am Bull 123:1427–1447
Lowrie W (2007) Fundamentals of geophysics, 2nd edn. Cambridge University Press, Cambridge
Maierová P, Chust T, Steinle-Neumann G et al (2012) The effect of variable thermal diffusivity on kinematic models of subduction. J Geophys Res 117:B07202
Maj S (2008) Remarks on the thermal conductivity and heat flow density of the Indian craton. Acta Geophys 56:994–999
Mancktelow NS (2008) Tectonic pressure: theoretical concepts and modeled examples. Lithos 103:149–177
Mandal N, Mitra AM, Bose S (2009) Orogenic processes in collision tectonics with a special reference to the Himalayan Mountain Chain: a review of theoretical and experimental models. Physics and chemistry of the earth's interior: crust, mantle and core, pp 41–66
Marques FO (2012) Modelling in geosciences. Tectonophysics 526–529:1–4
Marsh BD (1989) Magma physics. In: James DE (ed) The encyclopedia of solid earth geophysics. Van Nostrand Reinhold Company, New York, pp 676–689
Martin AJ, Ganguli J, DeCelles PG (2005) Metamorphism of Greater and Lesser Himalayan rocks exposed in the Modi Khola valley, central Nepal. Contrib Mineral Petrol 159:203–223
Matyska C, Yuen DA (2007) Lower mantle material properties and convection models of multi-scale plumes. In: Foulger GR, Jurdy DM (eds) Plates, Plumes and Planetary Processes. Geol Soc Am Spec Pap 430:137–163
McBirney AR (1994) Igneous petrology. CBS Publishers, New Delhi
McCall GJM (2005) Crust. In: Shelley RC, Cocks LRM, Pimer IR (eds) Encyclopedia of geology. Elsevier, Amsterdam, pp 403–409
Mizutani S (1984) Salt domes in the gulf coast. In: Uemura T, Mizutani M (eds) Geological structures. Wiley, Chichester, pp 106–133
Molli G, Iacopini D, Pertusati PC et al (2008) (internet reference) Architecture, strain features and fault rock types of the South Tibetan Detachment system between Katra and Tingri (South Tibet Himalaya). http://209.85.175.104/search?q=cache:DWXY1Ve5_T8J:www.see.leeds.ac.uk/peachandhorne/friday/047_Mollietal.pdf?Architecture,?strain?features?and?fault?rock?types?of?the?South?Tibetan?Detachment?system?betwe&hl=en&ct=clnk&cd=1&gl=in; http://www.env.leeds.ac.uk/peachandhorne/friday/047_Mollietal.pdf (Accessed on 1 May 2008
Morley CK (1988) Out-of-sequence thrusts. Tectonics 7:539–561
Mottram CM, Harris NBW, Parrish NB (2011) Shedding light on the Main Central Thrust Controversy, Sikkim Himalaya. J Him Earth Sci 44:6–61
Mouthereau F, Lacombe O, Vergés J (2012) Building the Zagros collisional orogen: timing, strain distribution and the dynamics of Arabia/Eurasia plate convergence. Tectonophysics 532–535: 27–60
Mukherjee S (2005) Channel flow, ductile extrusion and exhumation of lower-middle crust in continental collision zones. Curr Sci 89:435–436. http://www.iisc.ernet.in/currsci/aug102005/435.pdf
Mukherjee S (2007) Geodynamics, deformation and mathematical analysis of metamorphic belts of the NW Himalaya. Unpublished PhD thesis. Indian Institute of Technology Roorkee, pp 1–267
Mukherjee S (2009) Channel flow model of extrusion of the higher Himalaya-successes & limitations, vol 11. Geophysical Research Abstract, European Geosciences Union, Vienna, Austria, 19–24 April, EGU2009-13966
Mukherjee S (2010a) Structures at Meso- and Micro-scales in the Sutlej section of the Higher Himalayan Shear Zone in Himalaya. e-Terra 7:1–27
Mukherjee S (2010b) Microstructures of the Zanskar Shear Zone. Earth Sci India 3:9–27
Mukherjee S (2010c) Applicability of Channel flow as an extrusion mechanism of the Higher Himalayan Shear Zone from Sutlej, Zanskar, Dhauliganga and Gorigang Sections, Indian Himalaya. vol 12, EGU2010-14, 2010. Geophys Res Abs. EGU General Assembly 2010
Mukherjee S (2011a) Kinematics of "top-to-down" simple shear model in a Newtonian viscous rheology. Ind J Geophys Union (submitted)
Mukherjee S (2011b) Channel flow extrusion model to constrain viscosity and Prandtl number of the Higher Himalayan Shear Zone. Abstract. Tectonic Studies Group Annual Meeting. 04-06 January 2012, Edinburgh, UK
Mukherjee S (2011c) Tectonic problems in the Higher Himalayan Shear Zone, Bhagirathi section, Indian Himalaya. Int J Earth Sci Eng 4:411–417
Mukherjee S (2011d) Estimating the Viscosity of Rock Bodies - A Comparison Between the Hormuz- and the Namakdan Salt Diapirs in the Persian Gulf, and the Tso Morari Gneiss Dome in the Himalaya. J Ind Geophys Union 15:161–170
Mukherjee S (2012a) Simple shear is not so simple! Kinematics of Newtonian viscous simple shear zones. Geol Mag 149:819–826
Mukherjee S (2012b) Viscous dissipation pattern in incompressible Newtonian simple shear zones- analytical model & application in the Higher Himalaya. Int J Earth Sci (submitted)
Mukherjee S (2012c) A Microduplex. Int J Earth Sci 101:503
Mukherjee S (2012d) Mica inclusions inside host mica grains-examples from Sutlej section of the Higher Himalayan Shear Zone, India. J Earth Sci (in press)
Mukherjee (2012e) Tectonic implications and morphology of trapezoidal mica grains from the Sutlej section of the Higher Himalayan Shear Zone, Indian Himalaya. J Geol (in press)
Mukherjee S (2012f) Channel flow extrusion model to constrain viscosity and Prandtl number of the Higher Himalayan Shear Zone. Geophysical Research Abstracts Vol 14, EGU2012-3381, 2012 European Geosciences Union, General Assembly
Mukherjee S, Bandyopadhyay A (2011) Structural geology of the Bhagirathi section of the Higher Himalayan Shear Zone with special reference to back-thrusting. Abstract in "International Conference on Indian Monsoon and Himalayan Geodynamics". Wadia Institute of Himalayan Geology. Dehradun. India
Mukherjee S, Koyi HA (2010a) Higher Himalayan Shear Zone, Sutlej section: structural geology and extrusion mechanism by various combinations of simple shear, pure shear and channel flow in shifting modes. Int J Earth Sci 99:1267–1303
Mukherjee S, Koyi HA (2010b) Higher Himalayan Shear Zone, Zanskar Indian Himalaya—microstructural studies & extrusion mechanism by a combination of simple shear & channel flow. Int J Earth Sci 99:1083–1110
Mukherjee S, Mukherjee B (2012) Meeting Report: Session: "Geodynamics of Collision type orogenic belts and plateaus and its response to climate and erosional processes- Himalaya, Pamir, Central Asia and Tibet" TS 4.5: European Geosciences Union 2012, Vienna, Austria. J Geol Soc Ind (Submitted)
Mukherjee S, Mulchrone K (2012) Estimating the Viscosity of the Tso Morari Crystallines Gneiss Dome, Indian Western Himalaya. Int J Earth Sci (in press)
Mukherjee S, Talbot CJ, Koyi HA (2010) Viscosity estimates of salt in the Hormuz and Namakdan salt diapirs, Persian Gulf. Geol Mag 147:497–507
Mukherjee S, Koyi HA, Talbot CJ (2012) Implications of channel flow analogue models for extrusion of the Higher Himalayan Shear Zone with special reference to the out-of-sequence thrusting. Int J Earth Sci 101:253–272

Murphy MA, Harrison TM (1999) Relationship between leucogranites and the Qomolangma detachment in the Rongbuk valley, South Tibet. Geology 27:831–834

Nabelek PI, Whittington AG, Hofmeister AM (2010) Strain heating as a mechanism for partial melting and ultrahigh temperature metamorphism in convergent orogens: implications of temperature-dependent thermal diffusivity and rheology. J Geophys Res 115:B12417

Nabelek PI, Hofmeister AM, Whittington AG (2012) The influence of temperature-dependent thermal diffusivity on the conductive cooling rates of plutons and temperature-time paths in contact aureoles. Earth Planet Sci Lett 317–318:154–164

Natarov SI, Conrad CP (2012) The role of Poiseuille flow in creating depth-variation of asthenospheric shear. Geophys J Int (in press)

Neogi S, Dasgupta S, Fukuoka M (1998) High P-T polymetamorphism, dehydration melting, and generation of migmatites and granites in the Higher Himalayan Crystalline Complex, Sikkim, India. J Petrol 39:61–99

Olson P (1989) Mantle convection and plumes. In: James DE (ed) The encyclopedia of solid earth geophysics. Van Nostrand Reinhold Company, New York, pp 788–802

Oswald P (2009) Rheophysics: the deformation and flow of matter. Cambridge University Press, Cambridge

Pan SZ, Niu FL (2011) Large contrasts in crustal structure and composition between the Ordos plateau and the NE Tibetan plateau from receiver function analysis. Earth Planet Sci Lett 303:291–298

Papanastasiou CT, Georgiou GC, Lexandrou AN (2000) Viscous fluid flow. CRC Press, Florida

Park RG (1997) Foundations of structural geology, 3rd edn. Chapman & Hall, London

Patel RC, Carter A (2009) Exhumation history of the Higher Himalayan Crystalline along Dhauliganga-Goriganga river valleys, NW India: new constraints from fission track analysis. Tectonics 28:TC3004

Perchuk LL, Gerya TV (2011) Formation and evolution of Precambrian granulite terranes: a gravitational redistribution model. Geol Soc Am Mem 207:1–22

Petford N, Cruden AR, McCaffrey J-L et al (2000) Granite magma formation, transport and emplacement in the Earth's crust. Nature 408:669–673

Philpotts AR, Ague JJ (2009) Principles if igneous and metamorphic petrology. Cambridge University Press, Cambridge, pp 43, 567

Piffner OA (2006) Thick-skinned and thin-skinned styles of continental contraction. In: Mazzoli S, Butler RWH (eds) Styles of continental contraction. Geol Soc Am Spec Pap 414:153–177

Platt JP, Behr WM (2011) Lithospheric shear zones as constant stress experiments. Geology 39:127–130

Ponraj M, Miura S, Reddy CD et al (2011) Slip distribution beneath the Central and Western Himalaya inferred from GPS observations. Geophys J Int 185:724–736

Ramberg H (1981) Gravity, deformation and the Earth's crust in theory, experiments and geological applications, 2nd edn. Academic Press, London

Ramsay JG (1980) Shear zone geometry: a review. J Struct Geol 2:83–99

Ramsay JG, Lisle R (2000) The techniques of modern structural geology. Volume 3: applications of continuum mechanics in structural geology. Academic Press, San Francisco

Ray L, Förster H-J, Schilling FR et al (2006) Thermal diffusivity of felsic to mafic granulites at elevated temperatures. Earth Planet Sci Lett 251:241–253

Ray L, Bhattacharya A, Roy S (2007) Thermal conductivity of Higher Himalayan Crystallines from Garhwal Himalaya, India. Tectonophysics 434:71–79

Rey PF, Teysser C, Whiteney D (2010) Limit of channel flow in orogenic plateaux. Lithosphere 2:328–332

Robert X, van der Beek P, Braun J et al (2011a) Assessing Quaternary reactivation of the Main Central thrust zone (central Nepal Himalaya): new thermochronologic data and numerical modeling. Geology 37:731–734

Robert X, van der Beek P, Braun J et al (2011b) Control of detachment geometry on lateral variations in exhumation rates in the Himalaya: insights from low-temperature thermochronology and numerical modeling. J Geophys Res 116:B05202

Robinson D, DeCelles PG, Copeland P (2006) Tetconic evolution of the Himalayan thrust belt in western Nepal: implications for channel flow models. Geol Soc Am Bull 118:865–885

Rolfo F, Carosi R, Montomoli C et al (2008) Discovery of granulitized eclogite in North Sikkim expands the Eastern Himalaya high-pressure province. Extended abstracts: 23rd Himalayan-Karakoram-Tibet workshop, Leh, India. Him J Sci 5:126–127

Rosenberg CL, Medvedev S, Handy MR (2007) Effects of melting on faulting and continental deformation. In: Handy MR, Hirth G, Hovius N (eds) Tectonic faults- agents of change on a dynamic earth. The MIT Press, Cambridge, pp 317–401

Rutter EH, Mecklenburgh J, Brodie KH (2011) Rock mechanics constraints on mid-crustal low-viscosity flow beneath Tibet. In: Prior DJ, Rutter EH, Tatham DJ (eds) Deformation mechanisms, rheology and tectonics: microstructures, mechanics and anisotropy. Geol Soc, London, Sp Pub, 360:329–336

Sarkar RK, Saha DK (2006) A note on the lithosphere thickness and heat flow density of the Indian Craton from MAGSAT data. Acta Geophys 54:198–204

Scheidegger AE (1982a) Principles of geodynamics, 3rd edn. Springer, Berlin, pp 1–395

Scheidegger AE (1982b) Principles of geodynamics, 3rd edn. Springer, Berlin

Schlichting H, Gersten K (1999) Boundary layer theory, 8th revised enlarged edn. Springer, Berlin

Schultz-Ela DD, Walsh P (2002) Modeling of grabens extending above evaporites in Canyonlands National Park, Utah. J Struct Geol 24:247–275

Searle MP, Godin L (2003) The South Tibetan Detachment and the Manaslu Leucogranite: a structural reinterpretation and restoration of the Annapurna–Manaslu Himalaya, Nepal. J Geol 111:505–523

Searle MP, Szulc AG (2005) Channel flow and ductile extrusion of the High Himalayan Slab—the Kanchenjhunga-Darjeeling profile, Sikkim Himalaya. J Asian Earth Sci 25:173–185

Searle MP, Treloar PJ (2010) Was Late Cretaceous-Paleocene obduction of ophiolite complexes the primary cause of crustal thickening and regional metamorphism in the Pakistan Himalaya. In: Kusky TM, Zhai M-G, Xiao W (eds) The Evolving Continents: Understanding Processes of Continental Growth. Geol soc, London Spec Publ 338:345–359

Searle MP, Simpson RL, Law RD et al (2003) The structural geometry, metamorphic and magmatic evolution of the Everest massif, High Himalaya of Nepal-South Tibet. J Geol Soc Lond 160:345–366

Searle MP, Law RD, Jessup M (2006) Crustal structure, restoration and evolution of the Greater Himalaya in Nepal-South Tibet: implications for channel flow and ductile extrusion of the middle crust. In: Law RD, Searle MP (eds) Channel flow, extrusion and exhumation in continental collision zones. Geol Soc Lond Spec Publ 268:355–378

Searle MP, Law RD, Godin L et al (2008) Defining the Himalayan Main Central Thrust in Nepal. J Geol Soc Lond 165:523–534

Searle MP, Cottle JM, Streule MJ et al (2010) Crustal melt granites and migmatites along the Himalaya: melt source, segregation, transport and granite emplacement mechanisms. Earth Env Sci Trans R Soc Edinb 100:219–233

Searle MP, Elliot JR, Phillips RJ et al (2011) Crustal–lithospheric structure and continental extrusion of Tibet. J Geol Soc Lond 168:633–672

Seshunarayana T, Prasad BR, Prasad ASSRS et al (2011) Subsurface Structure Derived from Detailed Gravity and Magnetic Investigations along the Pala-Maneri Traverse of the Main Central Thrust, NW Himalaya. J Geol Soc Ind 77:213–218

Sharma RS (2009) Cratons and fold belts of India. Springer, Berlin, pp 130–131

Singh J, Park W-K, Yadav RR (2006) Tree-ring-based hydrological records for western Himalaya, India, since A.D. 1560. Clim Dyn 26:295–303

Spencer CJ, Harris RA, Dorais MJ (2011) Depositional provenance of the Himalayan metamorphic core of Garhwal region, India: constrained by U-Pb and Hf isotopes in zircons. Gond Res 22:26–35

Spencer CJ, Harris RA, Dorais MJ (2012) The metamorphism and exhumation of the Himalayan metamorphic core, eastern Garhwal region, India. Tectonics 31:TC1007

Spikings R, Dungan M, Foeken J et al (2008) Tectonic response of the central Chilean margin (35–388S) to the collision and subduction of heterogeneous oceanic crust: a thermochronological study. J Geol Soc Lond 165:941–953

Stacey FD (1969) Physics of the earth. Wiley, New York

St-Onge MR, Searle MP, Wodicka N (2006) Trans-Hudson Orogen of North America and Himalaya- Karakoram-Tibetan Orogen of Asia: Structural and thermal characteristics of the lower and upper plates. Tectonics 25:TC4006

Streule MJ, Strachan RA, Searle MP et al (2010) Comparing Tibet-Himalayan and Caladonian crustal architecture, evolution and mountain building processes. In: Law RD, Butler RWH, Holdsworth RE et al (eds) Continental tectonics and mountain building: the legacy of peach and hone. Geol Soc, London Spec Publ 335:207–232

Streule MJ, Carter A, Searle MP et al (2012) Constraints on brittle field exhumation of the Everest-Makalu section of the Greater Himalayan Sequence: implications for models of crustal flow. Tectonics 31:TC3010

Stüwe K (2007) Geodynamics of the Lithosphere, 2nd edn. Springer, Berlin

Sudha K, Tezkan B, Israil M et al (2011) Combined electrical and electromagnetic imaging of hot fluids within fractured rock in rugged Himalayan terrain. J Appl Geophys 74:205–214

Talbot CJ (1999) Can field data constrain rock viscosities? J Struct Geol 21:949–957

Talbot CJ, Aftabi P (2004) Geology and models of salt extrusion at Qum Kuh, central Iran. J Geol Soc Lond 161:321–334

Tanner DC (1999) The scale-invariant nature of migmatite from the Oberpfalz, NE Bavaria and its significance for melt transport. Tectonophysics 302:297–305

Tapponnier P (2012) The growth and rise of Tibet: a consequence of east Asian extrusion tectonics. Abstract in Asian Oceania Geosciences Society Joint Assembly 13–17 Aug 2012, Singapore. http://www.asiaoceania.org/aogs2012/doc/lecturers/SL/SE/SE1/SE1_Paul_TAPPONNIER_Abstract.pdf

Teysser C (2011) Exhumation of deep orogenic crust. Lithosphere 439–443

Thiede RC, Bookhagen B, Arrowsmith JR et al (2004) Climatic control on rapid exhumation along the Southern Himalayan Front. Earth Planet Sci Lett 202:791–806

Thiede RC, Ehlers TA, Bookhagen B et al (2009) Erosional variability along the northwest Himalaya. J Geophys Res 114:F01015

Thompson AB (1999) Some time-space relationships for crustal melting and granitic intrusion at various depths. In: Castro A, Fernández C, Vigneresse JL (Eds) Understanding granites: integrating new and classical techniques. Geol soc, London, Sp Pub 7–25

Tobgay T, MacQuarrie N, Long S et al (2012) The age and rate of displacement along the Main Central Thrust in the western Bhutan Himalaya. Earth Planet Sci Lett 319–320:146–158

Tolkunova TL (1977) Lithosphere viscosity from data on recent vertical and isostatic movements of the earth's crust. In: Mörner N-A (ed) Proceedings of earth rheology and late Cenozoic movement. Wiley, Chichester, pp 135–141

Turcotte DL, Schubert G (2002) Geodynamics, 2nd edn. Cambridge University Press, Cambridge, pp 48, 433, 435

Unsworth M (2010) Magnetotelluric studies of active continent–continent collisions. Surv Geophys 31:137–161

Vannay J-C, Grasemann B (2001) Himalayan inverted metamorphism and syn-convergence extension as a consequence of a general shear extrusion. Geol Mag 138:253–276

Vannay J-C, Grasemann B, Rahn M et al (2004) Miocene to Holocene exhumation of metamorphic crustal wedge in the NW Himalaya: evidence for tectonic extrusion coupled to fluvial erosion. Tectonics 23(TC1014):1–24

Vauchez A, Tommasi A, Mainprice D (2012) Faults (shear zones) in the Earth's mantle. Tectonophysics 558–559:1–27

Vergnolle M, Pollitz F, Calais E (2003) Constraints on the viscosity of the continental crust and mantle from GPS measurements and postseismic deformation models in western Mongolia. J Geophys Res 108:B10, 2502

Walker JD, Martin MW, Bowring SA et al (1999) Metamorphism, melting and extension: age constraints from the High Himalayan Slab of southeast Zanskar and northwest Lahaul. J Geol 107:473–495

Wang X, Zhang J, Santosh M et al (2012) Andean-type orogeny in the Himalayas of south Tibet: implications for early Paleozoic tectonics along the Indian margin of Gondwana. Lithos (in press)

Warren CJ, Beaumont C, Jamieson RA (2008a) Deep subduction and rapid exhumation: role of crustal strength and strain weakening in continental subduction and ultrahigh-pressure rock exhumation. Tectonics 27:TC6002

Warren CJ, Beaumont C, Jamieson RA (2008b) Modelling tectonic styles and ultra-high pressure (UHP) rock exhumation during the transition from oceanic subduction to continental collision. Earth Planet Sci Lett 267:129–145

Warren CJ, Beaumont C, Jamieson RA (2008c) Formation and exhumation of ultra-high pressure rocks during continental collision: role of detachment in the subduction channel. Geochem Geophys Geosyst 9:Q04019

Warren CJ, Grujic D, Kellett DA (2011) Probing the depths of the India-Asia collision: U-Th-Pb monazite chronology of granulites from NW Bhutan. Tectonics 30:2004

Watts AB (2001) Isostasy and flexure of the lithosphere. Cambridge University Press, Cambridge

Webb AAG, Yin A, Harrison TM et al (2011) Cenozoic tectonic history of the Himachal Himalaya (northwestern India) and its constraints on the formation mechanism of the Himalayan orogen. Geosphere 7:1013–1061

Whipp DM Jr, Ehlers TA, Todd A et al (2005) Kinematic and erosion history of the Greater Himalayan sequence, central Nepal, from integrated thermochronology and numerical modeling. Session 153. Thermochronology: techniques, applications and interpretations II. Geol Soc Am Prog 37:346

White LT, Lister LS (2012) The collision of India with Asia. J Geodyn 56–57:7–17

White LT, Ahmad T, Lister GS et al (2012) Is the switch from I- to S-type magmatism in the Himalayan Orogen indicative of the collision of India and Eurasia? Australian J Earth Sci 59:321–340

Whitney DL, Teyssier C, Rey PF (2009) The consequences of crustal melting in continental subduction. Lithosphere 1:323–327

Whittington AG, Hofmeister AM, Nabelek PI (2009) Temperature-dependent thermal diffusivity of the Earth's crust and implications for magmatism. Nature 458:319–321

Williams ML, Jercinovic J (2012) Tectonic interpretation of metamorphic tectonites: integrating compositional mapping, microstructural analysis and in situ monazite dating. J Meta Geol 30:739–752

Yakymchuk C, Godin L (2012) Coupled role of deformation and metamorphism in the construction of inverted metamorphic sequences: an example from far-northwest Nepal. J Meta Geol 30:513–535

Yakymchuk C, Harris L, Godin L (2012) Centrifuge modelling of deformation of a multi-layered sequence over a ductile substrate: 1. Style and 4D geometry of active cover folds during layer-parallel shortening. Int J Earth Sci 463–482

Yang J, Xu Z, Robinson PL et al (2011) HP-UHP Metamorphic Belts in the Eastern Tethyan Orogenic System in China. In: Dobrzhinetskaya LF, Faryad SW, Wallis S et al (eds) Ultrahigh-Pressure Metamorphism: 25 Years after the discovery of coesite and diamond. Part IV: Ultrahigh-pressure metamorphic belts and protolith history of eclogite and garnet peridotite. Elsevier, Amsterdam, pp 459–499

Yang Y, Ritzwoller MH, Zheng W et al (2012) A synoptic view of the distribution and connectivity of the mid-crustal low velocity zone beneath Tibet. J Geophys Res 117:B04303

Yin A (2006) Cenozoic tectonic evolution of the Himalayan orogen as constrained by along-strike variation of structural geometry, extrusion history, and foreland sedimentation. Earth Sci Rev 76:1–131

Yin A (2010) Cenozoic tectonic evolution of Asia: a preliminary synthesis. Tectonophysics 488:293–395

Yin A, Dubey CS, Kelty TK et al (2007) Construction of the eastern Himalaya by thick-skinned thrust stacking of the Indian basement: No lower crustal channel flow from Tibet is needed. Am Geophys Union Fall Meeting, Abstract # T34C-09

Zeitler PK, Melzer AS, Koons PO et al (2001) Erosion, Himalayan Geodynamics, and the Geomorphology of Metamorphism. GSA Today, pp 4–9

Zhang H, Harris N, Parrish R et al (2004) Causes and consequences of protracted melting of the mid-crust exposed in the North Himalayan antiform. Earth Planet Sci Lett 228:195–212

Zhang ZM, Zhao GC, Santosh M et al (2010) Two stages of granulite facies metamorphism in the eastern Himalayan syntaxis, south Tibet: petrology, zircon geochronology and implications for the subduction of Neo-Tethys and the Indian continent beneath Asia. J Meta Geol 28:719–733

Zhang J, Santosh M, Wang X et al (2012) Tectonics of the northern Himalaya since the India-Asia collision. Gond Res 21:939–960

Zhao W, Zhao X, Shi D et al (2004) Progress in the study of deep profiles of Tibet and the Himalayas (INDEPTH). Acta Geol Sinica 78:931–939

Zhu D, Meng X, Shao Z et al (2010) Upwelling process of the western Himalaya Mountains: height and velocity estimation evidenced by formation and evolution of the Zanda basin, Tibet, China. Acta Geol Scinica 84:280–295